보건학석사 학위논문

Source Apportionment and Oxidative Potential of $PM_{2.5}$ and $PM_{1.0}$ in Seoul

서울 $PM_{2.5}$와 $PM_{1.0}$의

오염원 추정과 산화 잠재력 평가

2022년 8월

서울대학교 대학원

환경보건학과 환경보건학전공

김태연

Source Apportionment and Oxidative Potential of $PM_{2.5}$ and $PM_{1.0}$ in Seoul

서울 $PM_{2.5}$와 $PM_{1.0}$의

오염원 추정과 산화 잠재력 평가

지도 교수 이승묵

이 논문을 보건학석사 학위논문으로 제출함

2022년 5월

서울대학교 대학원

환경보건학과 환경보건학전공

김태연

김태연의 보건학석사 학위논문을 인준함

2022년 7월

위 원 장 _____ 조경덕 _____ (인)

부위원장 _____ 허종배 _____ (인)

위 원 _____ 이승묵 _____ (인)

Abstract

Source Apportionment and Oxidative Potential of $PM_{2.5}$ and $PM_{1.0}$ in Seoul

Taeyeon Kim

Department of Environmental Health Sciences

Graduate School of Public Health

Seoul National University

Since $PM_{1.0}$ is mainly emitted from anthropogenic processes and contributes greatly to the health effects of $PM_{2.5}$, the need for research into $PM_{1.0}$ as well as $PM_{2.5}$ is growing. In this study, the constituents of $PM_{2.5}$ and $PM_{1.0}$ in Seoul were analyzed and the oxidative potential was measured by dithiothreitol (DTT) assay. The sources were identified by positive matrix factorization (PMF) and their characteristics were compared by conditional bivariate probability function (CBPF), cluster analysis, and potential source contribution function (PSCF). In the average mass concentration of 123 samples collected in Seoul, $PM_{1.0}$ (15.1 $\mu g/m^3$) accounted for about 75% of $PM_{2.5}$ (20.1 $\mu g/m^3$). This indicates that secondary sources and combustion-related sources mainly contribute to $PM_{2.5}$. The organic carbon (OC), SO_4^{2-}, and NH_4^+ fractions were significantly higher in $PM_{1.0}$ than in $PM_{2.5.}$ For the crustal elements, the fraction was significantly higher in $PM_{2.5}$ than in $PM_{1.0}$. In the result of the PMF model, ten sources contributed to $PM_{2.5}$ and $PM_{1.0}$, and each source and its contribution ($\mu g/m^3$) were as follows ($PM_{2.5}$, $PM_{1.0}$). Secondary nitrate: 6.01 (29%), 5.23 (32%); Secondary sulfate: 3.64 (17%), 3.48 (22%); Mobile: 2.71 (13%), 1.81

(11%); Biomass burning: 2.69 (13%), 2.03 (13%); Incinerator: 0.81 (3.8%), 0.69 (4.3%); Soil: 0.61 (2.9%), 0.30 (1.9%); Industry: 1.65 (7.8%), 0.40 (2.5%); Coal combustion: 1.77 (8.4%), 1.22 (7.6%); Oil combustion 0.40 (1.9%), 0.35 (2.2%); Aged sea salt: 0.72 (3.4%), 0.64 (4.0%). The fractional contributions (%) of secondary sources (secondary nitrate and secondary sulfate) in $PM_{1.0}$ were higher than in $PM_{2.5}$. For industry and soil sources, the fractional contributions were higher in $PM_{2.5}$ than in $PM_{1.0}$. In mobile source, there was a difference in constituents by road dust. The CBPF plots showed the direction of sources around Seoul. These plots showed that many sources were influenced from industrial complexes located in the south and the west of Seoul. For the cluster analysis, the contribution of biomass burning increased when backward trajectories flowed through Manchuria and North Korea. In the cluster flowing from Shandong Province, the contribution of secondary sources increased. Also, in PSCF, North China Plain including Shandong Province was mainly indicated as a possible source area of secondary sources, and the contributions of these sources increased significantly when high concentration events (HCEs) occurred. In particular, secondary sulfate from North China Plain contributed greatly to $PM_{1.0}$ when HCEs occurred during seasonal management period (SMP). The DTTv of $PM_{2.5}$ and $PM_{1.0}$ were 0.611 nmol/min/m^3 and 0.588 nmol/min/m^3, respectively. $PM_{1.0}$ contributed mostly to the oxidative potential of $PM_{2.5}$. In Pearson correlation analysis, OC showed the highest correlation with DTTv ($PM_{2.5}$: r=0.873, $PM_{1.0}$: r=0.786). By the multiple linear regression, secondary nitrate and biomass burning were selected as variables to represent DTTv in both $PM_{2.5}$ and $PM_{1.0.}$ In this result, biomass burning was an important source related to oxidative potential and secondary nitrate showed the influence of secondary formation process. This study showed that the continuous studies of $PM_{1.0}$ were necessary to understand the characteristics of sources and oxidative potential, and showed that management of secondary sources and biomass burning source in Seoul was necessary.

Keyword: $PM_{2.5}$, $PM_{1.0}$, PMF (positive matrix factorization), PSCF (potential source contribution function), DTT (dithiothreitol) assay

Student Number: 2020-20432

Table of Contents

1. Introduction

$PM_{2.5}$ is particulate matter less than or equal to 2.5 μm in aerodynamic diameter, and it is mainly emitted from secondary formation, mobile, combustion, etc. Seoul, Korea, is a large city, and high concentration events of $PM_{2.5}$ steadily occur (E. H. Park et al. 2020). $PM_{2.5}$ in Seoul has large contributions of secondary sources and anthropogenic sources, and is influenced from the industrial complex and farmland in Gyeonggi-do. In addition, there is an influence of long-range transport from China and Mongolia (H. Kim, Zhang, and Heo 2018; Y. Kim et al. 2018; J. B. Heo, Hopke, and Yi 2009; J. Park et al. 2022; B. M. Kim et al. 2016).

$PM_{2.5}$ penetrates deep into the lungs and is known to be associated with cardiovascular and respiratory diseases (Araujo and Nel 2009; J. Heo et al. 2014). In addition, $PM_{2.5}$ increases reactive oxygen species (ROS) in the body. When ROS exceeds antioxidant capacity, it causes oxidative stress that causes inflammation. Therefore, the oxidative potential of particulate matter (PM) which increases ROS has been widely used to evaluate the health effect of $PM_{2.5}$ (J. Park et al. 2018; Ray, Huang, and Tsuji 2012; Bates et al. 2015; Vreeland et al. 2017). It is known that this oxidative potential is related to secondary organic aerosol (SOA) and transition metals in PM, and a study using the PMF (Positive matrix factorization) model showed that it was related to secondary aerosol and biomass burning (Verma et al. 2015; Jiang et al. 2019). In South Korea, it was observed that the oxidative potential increased when long-range transport such as Asian dust occurred (B. J. Lee et al. 2020). Due to these health effects, management for $PM_{2.5}$ is necessary. Accordingly, in Korea, National Ambient Air Quality Standard of $PM_{2.5}$ is set and managed. In addition, for management intensively, the seasonal management period is designated during winter when many high concentration events occur.

Recently, the need for research into $PM_{1.0}$ as well as $PM_{2.5}$ continues to be presented (H. Kim et al. 2017; Yanyun Zhang et al. 2018). $PM_{1.0}$ is particulate matter less than or equal to 1.0 μm in aerodynamic diameter. It is a part of $PM_{2.5}$, but it is different from $PM_{2.5\text{-}1.0}$ in the characteristics of sources, chemical composition, and

its effects. Since $PM_{1.0}$ is mainly emitted from anthropogenic activities such as incineration, it has higher ratio of constituents (secondary inorganic aerosol, organic carbon, and elemental carbon) mainly emitted from anthropogenic activities than for $PM_{2.5}$ (Farina et al. 2013; Samek et al. 2018; Yanyun Zhang et al. 2018). In addition, the small particles can pass through the air-blood barrier of the lungs and have a higher surface area per mass (Samek et al. 2018). Some study shows that ultrafine particles are the main reason for cardiovascular disease caused by atmospheric particles (Franck et al. 2011). Moreover, in toxicological analysis, a major influence on lung injury was from $PM_{1.0}$, and epidemiologic studies also emphasize the health effects of $PM_{1.0}$ (G. Chen et al. 2017; G. Wang et al. 2021). Because of these characteristics, it is necessary to study $PM_{1.0}$ as well as $PM_{2.5}$ to effectively manage PM. In particular, identifying sources and calculating the quantitative source contribution for $PM_{2.5}$ and $PM_{1.0}$ will contribute to comparing the characteristics of sources with each other. In addition, it is known that $PM_{1.0}$ has a large influence on health. Thus, it is important to understand how much $PM_{1.0}$ within $PM_{2.5}$ contribute to health effects such as the oxidative potential and which sources mainly contribute to health effects. This is necessary to control the source of PM in terms of public health. However, there is not enough studies of $PM_{1.0}$ in Korea. In particular, few studies have analyzed many constituents and identified the source based on filter data.

Therefore, the purpose of this study is to identify the sources of $PM_{2.5}$ and $PM_{1.0}$ in Seoul and to compare characteristics of not only source but also health effects with each other. For this, various chemical analyses were used to compare the constituents of $PM_{2.5}$ with those of $PM_{1.0}$, and the characteristics of each source were identified by the PMF (Positive matrix factorization) model. The health effects were verified by measuring the oxidative potential using the dithiothreitol (DTT) assay. In addition, multiple linear regression was applied to identify which source more contribute to health effect. Furthermore, the characteristics of sources according to specific events such as seasonal management period (SMP) and high concentration events (HCEs) were compared.

2. Method

2.1 Description of sampling site and procedure

Samples were collected on the roof (about 27 m above ground) of the Graduate school of Public Health building at Seoul National University (37.46° N, 126.95° E), Seoul, Korea. Seoul National University is located in Gwanak-gu, Seoul, with residential complexes and urban highways. It is the southwestern part of Seoul, close to Gyeonggi-do, where factories and industrial complexes are located. For each $PM_{2.5}$ and $PM_{1.0}$, 126 samples were collected every other day from June 5, 2021 to February 28, 2022. However, the period from August 20 to September 6 was excluded due to building maintenance. Samples were collected for 23 hours from 11:00 a.m. to 10:00 a.m. the next day.

The three-channel low-volume air samplers were used for sampling. Each channel consisted of a filter pack (URG-2000-30FG, URG, USA) and a cyclone (URG-2000-30EH and URG-2000-30EHB, URG, USA), and two types of Teflon filters (PTFE, MTL, UK; PTFE, Pall Corporation, USA) and a quartz filter (quartz microfiber filter, Pall Corporation, USA) were used. The flow rate of the low-volume air sampler was 16.7 L/min. From December 2021 to February 2022, which is a seasonal management period during the sampling period, 45 high-volume samples were additionally collected using high-volume air samplers (TE-HVPLUS, TISCH, USA) with impactor filter (TE-230-QZ, TISCH, USA). The high-volume air sampler had a flow rate of 40 ft^3/min and used quartz filter for sample collection. Two types of cyclones (low-volume air sampler) and additional impactor stages (high-volume air sampler) were used to collect $PM_{2.5}$ and $PM_{1.0}$.

2.2 Chemical analyses

Samples collected on a Teflon filter (MTL) were used for mass concentration and trace element analysis. The mass concentration was measured using a semi-micro balance (CP225D, Sartorius, Germany) with an accuracy of 10^{-5} g under the constant temperature (21.5 ± 1.5°C) and humidity (35 ± 5%).

The concentrations of 17 trace elements (Mg, Al, Si, Ca, Ti, V, Cr, Mn, Ba, Fe, Ni, Cu, Zn, As, Se, Br, and Pb) were analyzed using an energy dispersive X-ray fluorescence (EDXRF) spectrometer (EDXRF Spectrometer, Thermo Fisher, USA). The concentration of crustal elements among trace elements was calculated using the Equation (1) (Miller-Schulze et al. 2015).

$$\begin{aligned}[\text{Crustal elements}] &= 1.889[Al] + 1.400[Ca] + 1.430[Fe] + 1.658[Mg] \\ &+ 1.582[Mn] + 2.139[Si] + 1.668[Ti]\end{aligned} \quad (1)$$

Samples collected on another Teflon filter (Pall Corporation) was used for ionic species analysis. Samples were extracted with distilled water (resistivity=18.2 MΩ·cm) and filtered using a 0.2 μm syringe filter. After that, ionic species (NO_3^-, SO_4^{2-}, Cl^-, NH_4^+, Na^+, and K^+) were analyzed using ion chromatography (ICS-1100, Thermo Fisher Scientific, USA).

Samples collected on a quartz filter were used for carbonaceous species (OC: organic carbon, EC: elemental carbon) analysis. OC and EC were analyzed using a carbon aerosol analyzer (Model 5L, Sunset Laboratory Inc., USA) which uses the thermal optical transmittance (TOT) method following the National Institute for Occupational Safety and Health (NIOSH) 870 protocol. The details of analytical methods and pretreatment process followed previous studies (S. Kim et al. 2018; J. Park et al. 2018).

2.3 Source apportionment using PMF (Positive matrix factorization)

In this study, EPA's PMF 5.0, which has already been used in many studies, was used for the source apportionment (Khan et al. 2021; Yanyun Zhang et al. 2018; J. Park et al. 2022; J.-M. Park, Lee, and Kim 2022). The PMF (Positive matrix factorization) model is a receptor model based on least squares method and a progressed Factor Analysis model (J. B. Heo, Hopke, and Yi 2009; S. Kim et al.

2018). The equation of PMF is as shown in Equation (2) and Equation (3) below, and the objective of PMF is finding a solution that minimizes the Q value.

$$e_{ij} = x_{ij} - \sum_{k=1}^{p} f_{kj} g_{ik} \quad (2)$$

$$\mathrm{Q(E)} = \sum_{j=1}^{m} \sum_{i=1}^{n} \left[\frac{e_{ij}}{s_{ij}}\right]^2 \quad (3)$$

In Equation (2), j is species, i is samples, and k is sources. x_{ij} is the concentration of the jth species measured in the ith sample, g_{ik} is the kth source contribution in the ith sample, and f_{kj} is the mass species fraction from the jth species in the kth source. In Equation (3), e_{ij} is residual associated with the jth species of the ith sample and s_{ij} is the uncertainty estimated in the jth species of the ith sample.

Concentration and uncertainty data are required for input data of the PMF model. The uncertainty was calculated as shown in Table S1. If the concentration was below the detection limits (MDL), the concentration and uncertainty were replaced by 1/2 of the MDL and 5/6 of the MDL, respectively (J. Park et al. 2022).

A total of 26 species including the mass concentration of $PM_{2.5}$ or $PM_{1.0}$ were used. The mass concentration was set as a total variable, and species with low signal to noise ratio were selected as 'weak'. To find the optimal number of factors, the PMF model was run multiple times changing the number of factors from six factors to ten factors. In both $PM_{2.5}$ and $PM_{1.0}$, ten factors were selected based on the separation of the sources and the interpretability of the profile. In addition, displacement (DISP) analysis was performed for error estimation. The DISP is a good screening method to check the solution of the PMF model. Species with wide DISP interval are not significantly related to the factor because they can be removed with a rotation that would not significantly change the Q value of the solution. By checking the DISP

interval, especially the interval of the marker species of the source, uncertain judgment can be avoided in identifying the sources (J. Park et al. 2022; Brown et al. 2015). The principle and detailed method of the PMF model are the same as those described in previous studies (J. B. Heo, Hopke, and Yi 2009; S. Kim et al. 2018).

2.4 Conditional bivariate probability function (CBPF)

The conditional bivariate probability function (CBPF) was performed using wind direction and wind speed data to identify the location of local sources. The CBPF plots were obtained using the R Openair package. The basic equation is as Equation (4) below.

$$\mathrm{CBPF} = \frac{m_{\Delta\theta,\Delta u}}{n_{\Delta\theta,\Delta u}} \quad (4)$$

$n_{\Delta\theta,\Delta u}$ is the total number of data in the wind sector ($\Delta\theta$) with wind speed (Δu). $m_{\Delta\theta,\Delta u}$ is the number of occurrences with higher concentration than the threshold at that time (Uria-Tellaetxe and Carslaw 2014). The upper 25th percentile of the source contribution was set as the threshold criteria. Wind direction and wind speed data were obtained from the Korea Meteorological Administration's website (http://www.kma.go.kr).

2.5 Cluster analysis using backward trajectory

HYbrid Single Particle Lagrangian Integrated Trajectory 4 (HYSPLIT 4) model of the National Oceanic and Atmospheric Administration (NOAA) was used to generate backward trajectories from the sampling site. It is widely used to identify the air parcel trajectories flowing into the sampling site. In this study, 96 h backward trajectories calculated hourly were used and starting height was set to half the mixing height above ground level. The GDAS 1° from the Global Data Assimilation System (GDAS) was used as the meteorological data with a resolution of 1°. These backward trajectories during the sampling period were classified into several groups with similar speeds and directions by cluster analysis of HYSPLIT 4, and their characteristics were compared.

2.6 Potential source contribution function (PSCF)

The Potential source contribution function (PSCF) model is a method used in many studies to identify possible source areas and long-range transport (Zong et al. 2018; C. Chen et al. 2020; J. B. Heo, Hopke, and Yi 2009). In this study, the PSCF model was performed using the source contribution from PMF and backward trajectories generated from the HYSPLIT 4 model. The PSCF model is a conditional probability and is calculated as the number of endpoints whose source contribution is higher than the threshold value among the total number of endpoints of the backward trajectories passing the grid cell. The equation of PSCF is as Equation (5) below.

$$\mathrm{PSCF} = \frac{m_{ij}}{n_{ij}} \tag{5}$$

In Equation (5), n_{ij} is the total number of endpoints that passed the ijth grid cell and m_{ij} is the number of endpoints that pass the ijth cell when the source contributions are higher than the threshold value. In this study, the threshold value was set to the upper 25th percentile of the source contribution. In addition, a weight function was applied as in Equation (6) to reduce uncertainty from the small n_{ij} value (S. Kim et al. 2018).

$$\mathrm{W} = \begin{Bmatrix} 1.0, & (n > 3n_{avg}) \\ 0.8, & (2n_{avg} < n \leq 3n_{avg}) \\ 0.6, & (n_{avg} < n \leq 2n_{avg}) \\ 0.4, & (0.5n_{avg} < n \leq n_{avg}) \\ 0.2, & (n \leq 0.5n_{avg}) \end{Bmatrix} \tag{6}$$

2.7 Dithiothreitol (DTT) assay

Cellular and acellular methods have been used to measure the oxidative potential of particulate matter. Among acellular methods, the dithiothreitol (DTT) assay is an economical and quick method to obtain results and has been studied for its relevance to pathology. Therefore, DTT assay was widely used to measure the oxidative potential of particulate matter (Bates et al. 2019; Strak et al. 2017; B. J. Lee et al. 2020).

The DTT assay is performed in the order of extraction, DTT oxidation step, and DTT determination step. High-volume samples collected using a high-volume air sampler were extracted in 15 ml of distilled water and sonicated for 1 h. In the DTT oxidation step, 3.5 ml of the extracted solution was loaded into a vial, 1 ml of potassium phosphate buffer (0.5 M) and 0.5 ml of DTT (1 mM) were added, and incubated at 37°C. In the DTT determination step, 100 µl of the mixed solution was aliquoted and transferred to another vial at a set time (4 min, 13 min, 23 min, 30 min, and 41 min), and 1 ml of Trichloroacetic acid (TCA, 1% w / v) was added to the vial to quench the reaction. After that, 2 ml of Tris-HCl buffer (0.08 M) and 0.5 ml of 5,5'-dithiobis-(2-nitrobenzoic acid) (DTNB, 0.2 mM) were added to react the residual DTT with DTNB. When DTT reacts with DTNB, 2-nitro-5-thiobenzoic acid (TNB) which has an extinction coefficient of 14150 M^{-1} cm^{-1} at 412 nm wavelength is produced. The absorbance of TNB was measured at 412 nm wavelength using a UV/VIS spectrophotometer (SPECORD 50 plus, Analytik jena, Germany).

The DTT consumption rate was calculated using the absorbance measured at each time. The consumption rate normalized by air volume was calculated according to Equation (7) and Equation (8).

$$\sigma\mathrm{DTT} = -\sigma Abs \times \frac{N_0}{Abs_0} \tag{7}$$

$$DTTv = \frac{\sigma\mathrm{DTT}_{sample} - \sigma\mathrm{DTT}_{blank}}{V_t \times \frac{A_h}{A_t} \times \frac{V_S}{V_e}} \quad (8)$$

In Equation (7), σDTT (nmol/min) is the DTT consumption rate, and the slope (σAbs, Abs/min) and the intercept (Abs_0, Abs) of linear regression of absorbance and time were used. N_0 (nmol) is the moles of DTT added. In Equation (8), σDTT_{sample} (nmol/min) is the DTT consumption rate of the sample, σDTT_{blank} (nmol/min) is the DTT consumption rate of the blank sample, V_t (m^3) is air volume, A_h (cm^2) is the filter area used for extraction, A_t (cm^2) is the total area of the filter, V_s (ml) is the volume used for the reaction in the extraction solution, V_e (ml) is the volume used for extraction, and DTTv (nmol/min/m^3) is the DTT consumption rate normalized by air volume. In this study, the preparation of reagents and the assay were conducted according to previous study (Fang et al. 2015).

3. Results and Discussion

3.1 Chemical constituents

For each $PM_{2.5}$ and $PM_{1.0}$, 123 samples were selected in consideration of flow error, and chemical constituents of the samples were analyzed. The average concentration and standard deviation during the sampling period for each constituent are presented in Table 1.

The average mass concentrations of $PM_{2.5}$ and $PM_{1.0}$ during the sampling period were 20.1 (± 14.1) $\mu g/m^3$ and 15.1 (± 10.2) $\mu g/m^3$, respectively. High concentration events (HCEs) when $PM_{2.5}$ mass concentrations exceeded 24 h $PM_{2.5}$ National Ambient Air Quality Standard (NAAQS) in South Korea (35 $\mu g/m^3$) occurred in 16 samples during this period. The average $PM_{1.0}/PM_{2.5}$ ratio was 0.75 (± 0.12). Compared with other studies, the average $PM_{1.0}/PM_{2.5}$ ratio in Seoul was higher than the winter period ratios of Yinglite (0.60) and Baofeng (0.59) which are industrial regions of China and the ratio of Tianjin (0.63), an industrial port city. It was similar to the ratios of urban areas such as Beijing (0.794) and Shanghai (0.80) (Khan et al. 2021; Liang et al. 2019; Qiao et al. 2015; Yanyun Zhang et al. 2018). This high $PM_{1.0}/PM_{2.5}$ ratio indicated that $PM_{2.5}$ was mostly influenced by combustion-related sources and secondary aerosol sources that mainly contribute to the formation of small particles (G. Chen et al. 2018).

For each constituent of $PM_{2.5}$ and $PM_{1.0}$, the overall concentration was higher in $PM_{2.5}$, but there was a difference in each constituent fraction. In particular, there was a difference in OC, NO_3^-, SO_4^{2-}, NH_4^+, and crustal elements.

The average OC concentrations of $PM_{2.5}$ and $PM_{1.0}$ were 4.64 $\mu g/m^3$ and 4.00 $\mu g/m^3$, respectively, and the average EC concentrations were 0.31 $\mu g/m^3$ and 0.28 $\mu g/m^3$, respectively. In $PM_{2.5}$, about 86% of OC and about 90% of EC corresponded to $PM_{1.0}$, which were higher than the $PM_{1.0}/PM_{2.5}$ mass concentration ratio. In the concentration fraction, the OC fraction in $PM_{2.5}$ was about 23% and the OC fraction in $PM_{1.0}$ was 26%, indicating that the OC fraction in $PM_{1.0}$ was higher. The result of

the t-test indicated significant difference ($P<0.001$). Because OC is mainly emitted from the combustion process, the higher OC fraction in $PM_{1.0}$ than $PM_{2.5}$ indicates that combustion-related sources greatly contribute to $PM_{1.0}$ (Khan et al. 2021).

In the case of ionic species, the concentrations of NO_3^-, SO_4^{2-}, and NH_4^+ were 4.99 $\mu g/m^3$, 3.11 $\mu g/m^3$, 2.57 $\mu g/m^3$ for $PM_{2.5}$, 4.07 $\mu g/m^3$, 2.65 $\mu g/m^3$, and 2.19 $\mu g/m^3$ for $PM_{1.0}$. The $PM_{1.0}$ fraction of $PM_{2.5}$ were 82% in NO_3^-, 85% in SO_4^{2-}, and 85% in NH_4^+ which were higher than the ratio calculated as the mass concentration. The NO_3^-, SO_4^{2-}, and NH_4^+ fractions in $PM_{2.5}$ were 25%, 15%, and 13%, and 27%, 18%, and 14% in $PM_{1.0}$. From the t-test, the SO_4^{2-} and NH_4^+ fractions were significantly higher in $PM_{1.0}$ ($P<0.01$), but there was no significant difference in NO_3^-. These constituents were mainly related to secondary inorganic aerosols, and the highest average ratio of these constituents in particulate matter was observed in the size of 0.49 µm - 0.95 µm (Long et al. 2014).

In the case of crustal elements, $PM_{2.5}$ and $PM_{1.0}$ were 2.27 $\mu g/m^3$ and 0.60 $\mu g/m^3$, respectively. The crustal elements fraction in $PM_{2.5}$ accounted for 11% of the total concentration, whereas for $PM_{1.0}$, the fraction was 4.0%. This difference in fraction was significant ($P<0.001$). This indicated that the large particles had high crustal elements fraction. This is likely because the particles emitted from natural and mechanical processes are relatively large (Khan et al. 2021). Other low-concentration constituents showed similar levels in $PM_{2.5}$ and $PM_{1.0}$.

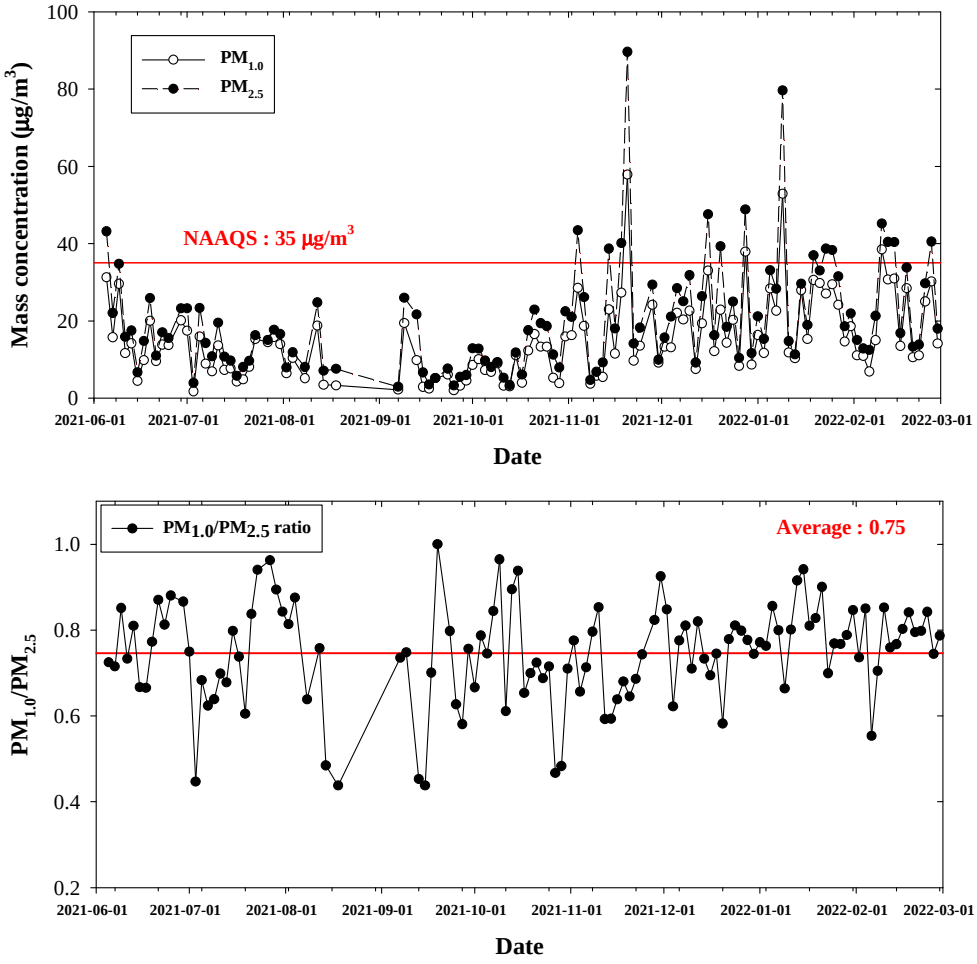

Figure 1 Time series of mass concentrations of $PM_{2.5}$ and $PM_{1.0}$, and $PM_{1.0}/PM_{2.5}$ ratio

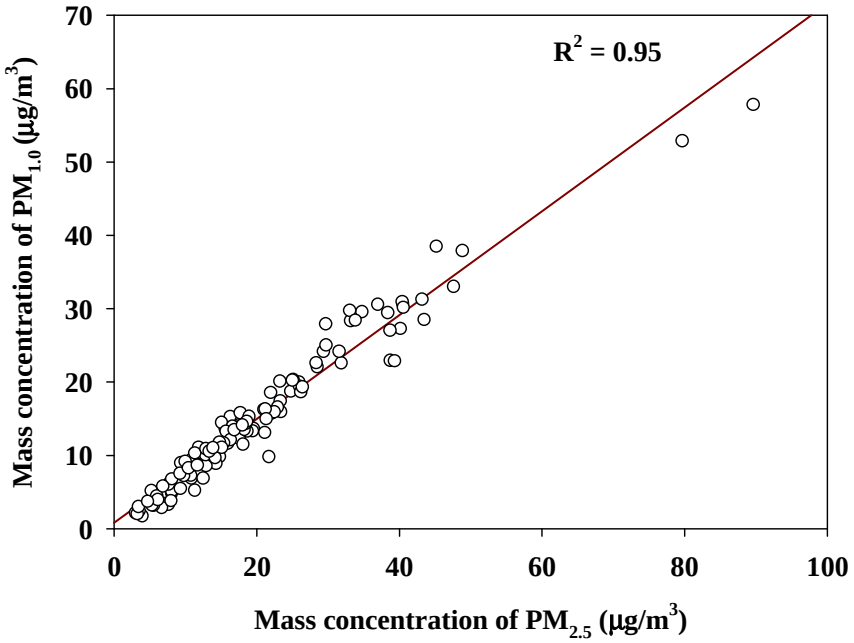

Figure 2 Scatterplot of mass concentrations of $PM_{2.5}$ and $PM_{1.0}$

Table 1 Summary of chemical constituents of $PM_{2.5}$ and $PM_{1.0}$

		$PM_{2.5}$		$PM_{1.0}$	
Species	Unit	Avg.	Stdev.	Avg.	Stdev.
Mass concentration	$\mu g/m^3$	20.1	14.1	15.1	10.2
OC	$\mu g/m^3$	4.64	2.26	4.00	1.94
EC	$\mu g/m^3$	0.31	0.17	0.28	0.14
NO_3^-	$\mu g/m^3$	4.99	6.04	4.07	4.66
SO_4^{2-}	$\mu g/m^3$	3.11	2.01	2.65	1.58
Cl^-	$\mu g/m^3$	0.41	0.31	0.32	0.22
NH_4^+	$\mu g/m^3$	2.57	2.51	2.19	1.93
Na^+	$\mu g/m^3$	0.22	0.31	0.18	0.24
K^+	$\mu g/m^3$	0.18	0.11	0.16	0.09
Σ Trace element	$\mu g/m^3$	1.48	0.81	0.47	0.25
Crustal	$\mu g/m^3$	2.27	1.33	0.60	0.31
Non-crustal	$\mu g/m^3$	0.19	0.12	0.13	0.13
Mg	ng/m^3	65.8	37.3	13.7	9.9
Al	ng/m^3	183.6	107.0	57.3	19.4
Si	ng/m^3	463.5	317.4	111.2	73.7
Ca	ng/m^3	180.0	108.9	26.2	14.8
Ti	ng/m^3	17.7	9.6	3.7	2.1
V	ng/m^3	1.2	0.9	1.0	0.9
Cr	ng/m^3	3.5	2.0	1.8	1.1
Mn	ng/m^3	20.3	11.1	12.2	6.9
Ba	ng/m^3	18.2	12.6	3.1	3.5
Fe	ng/m^3	358.4	188.2	121.3	68.0
Ni	ng/m^3	2.2	0.9	2.0	0.7
Cu	ng/m^3	15.9	9.4	10.1	6.8
Zn	ng/m^3	90.5	83.9	63.0	114.5
As	ng/m^3	11.1	13.4	5.8	5.6
Se	ng/m^3	2.5	2.1	2.4	2.0
Br	ng/m^3	18.1	12.8	16.2	10.4
Pb	ng/m^3	31.6	22.0	22.2	14.2

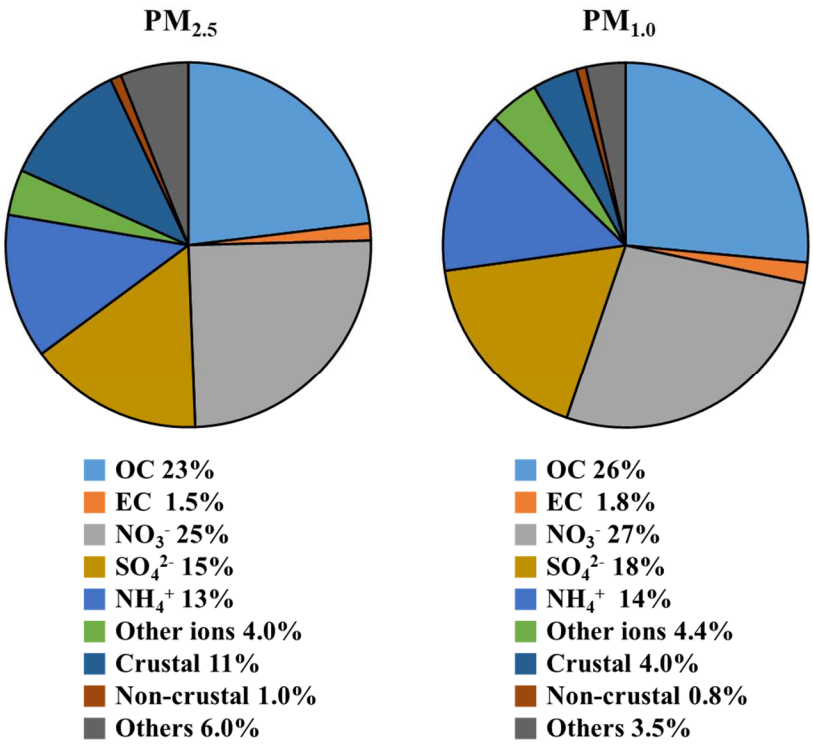

Figure 3 The chemical constituents fractions in $PM_{2.5}$ and $PM_{1.0}$

3.2 Source apportionment

In this study, ten factors contributed to $PM_{2.5}$ and $PM_{1.0}$ in Seoul. The factors were identified by high loadings and narrow DISP intervals of some constituents, and named based on the results of previous studies conducted in Seoul (J. B. Heo, Hopke, and Yi 2009; E. H. Park et al. 2020; J. Park et al. 2022). For both $PM_{2.5}$ and $PM_{1.0}$, ten factors were Secondary nitrate, Secondary sulfate, Mobile, Biomass burning, Incinerator, Soil, Industry, Coal combustion, Oil combustion, and Aged sea salt. The source profiles and the daily source contributions of $PM_{2.5}$ and $PM_{1.0}$ are presented in Figure 4 ~ Figure 7.

In order to statistically compare the seasonality of the sources, in this study, the period was divided into seasonal management period (SMP) of South Korea including the winter season (from December 2021 to February 2022) and Non-SMP, including the summer and autumn season (from June 2021 to November 2021). t-test result of each source is presented in Table 2.

Secondary nitrate source was identified by high loadings and narrow DISP intervals of NO_3^- and NH_4^+. It indicated that NO_3^- formed in the chemical transformation of NO_X to HNO_3 reacted with NH_3 to form NH_4NO_3 (Long et al. 2014; Waked et al. 2014). The average contributions ($\mu g/m^3$) of secondary nitrate source in $PM_{2.5}$ and $PM_{1.0}$ were 6.01 $\mu g/m^3$ (29%) and 5.23 $\mu g/m^3$ (32%), respectively. Secondary nitrate source greatly contributed to both $PM_{2.5}$ and $PM_{1.0}$. The contribution of secondary nitrate source in SMP was significantly higher than in Non-SMP. This was likely because the formation of secondary nitrate mainly occurs at low temperatures, and this trend was also observed in previous studies (S. Kim et al. 2018; J. Park et al. 2022).

Secondary sulfate source had the second highest contribution. The average contributions of secondary sulfate in $PM_{2.5}$ and $PM_{1.0}$ were 3.64 $\mu g/m^3$ (17%) and 3.48 $\mu g/m^3$ (22%), respectively. Secondary sulfate source was identified by high loadings and narrow DISP intervals of SO_4^{2-} and NH_4^+. The previous studies indicated that SO_2 was oxidized to H_2SO_4 and SO_4^{2-} in fine particles mostly existed

as $(NH_4)_2SO_4$ (D. Wang et al. 2016; Long et al. 2014). The oxidation to H_2SO_4 was enhanced by the strong photochemical reaction (S. Kim et al. 2018). Thus, the contribution of secondary sulfate source was high not only in SMP but also in Non-SMP.

Both secondary nitrate and secondary sulfate sources showed higher fractional contribution (%) in $PM_{1.0}$ than in $PM_{2.5}$. This was supported by the results of the study showing that the sulfur oxidation ratio and nitrogen oxidation ratio were high in particles smaller than 0.95 μm and more secondary sulfate and nitrate were formed in size of 0.49 μm - 0.95 μm (Long et al. 2014). The CBPF plots in Figure 8 and Figure 9 shows that both secondary nitrate and secondary sulfate sources mainly flow in from the southwest direction of Seoul, and the influence mainly appears when the wind speed is high. Thus, this indicates that there is an influence not only from the local sources but also from the distant location. Secondary nitrate and secondary sulfate sources were likely to be influenced by the gas-phase chemicals emitted from the coal-fired power plants and Yeongdong Expressway where located in the southwest direction of Seoul (J. Park et al. 2022).

Mobile source was identified by high loadings and narrow DISP intervals of OC and EC. In $PM_{2.5}$, additionally Ca, Cr, Ba, Fe, and Cu had high loadings and narrow DISP intervals, and for $PM_{1.0}$, Ba additionally had high loading and narrow DISP interval. The average contributions of this source in $PM_{2.5}$ and $PM_{1.0}$ were 2.71 $\mu g/m^3$ (13%) and 1.81 $\mu g/m^3$ (11%), respectively. OC and EC are known to be mainly emitted from the exhaust of vehicle (Lin et al. 2020). Ca and Fe are emitted from the resuspension of the road soil, and Cr, Ba, Fe, and Cu are emitted from the wearing of brake linings. In this study, these constituents showed high loadings in $PM_{2.5}$ and were used as markers of mobile source, but were not high in $PM_{1.0}$ except Ba (Thorpe and Harrison 2008; S. C. Lee et al. 2006). According to Iijima et al (2007), the peak value of the number concentration of particulate matter emitted from brake wear was found in 1-2 μm in diameter. In the CBPF, since its value appears high when the wind speed is low, mobile source is mainly influenced from local sources of Seoul rather than an inflow from the outside. However, for $PM_{1.0}$, it shows that there is

some inflow from the roads around Seoul such as Yeongdong Expressway. Unlike in $PM_{1.0}$, this appearance in $PM_{2.5}$ concentrated in the center may be due to influence of road dust which is large in the urban area and larger in $PM_{2.5}$ than in $PM_{1.0}$ (Apeagyei, Bank, and Spengler 2011; Hueglin et al. 2005).

Biomass burning source including crop residue burning and wood combustion was identified by high loadings and narrow DISP intervals of K^+, OC, and EC, known as makers of this source (Fourtziou et al. 2017; F. Duan et al. 2004; Yanyan Zhang et al. 2013; Jung et al. 2014). The average contributions of this source in $PM_{2.5}$ and $PM_{1.0}$ were 2.69 $\mu g/m^3$ (13%) and 2.03 $\mu g/m^3$ (13%), respectively. Biomass burning source was significantly high during SMP, and in other studies, the increase in biomass burning during winter in Seoul is explained by the influence of transported biomass burning sources from open burning and farm waste burning in the surrounding area (Y. Kim et al. 2018; E. H. Park et al. 2020; Choi et al. 2013). In the CBPF plot, the northwest direction is mainly shown, and in the case of $PM_{2.5}$, the southwest direction is also shown. This indicates that there were regional transports from agricultural land located around Seoul (Y. Kim et al. 2018; J. Park et al. 2022).

The average contributions of incinerator source in $PM_{2.5}$ and $PM_{1.0}$ were 0.81 $\mu g/m^3$ (3.8%) and 0.69 $\mu g/m^3$ (4.3%), respectively and Cl^- had high loading and narrow DISP interval in this source. Other studies also described this constituent as a marker of incinerator source, and Cl^- is mainly emitted from the treatment of wastes containing polyvinyl chloride and foods containing salt (H. H. Yang et al. 2016; J.-M. Park, Lee, and Kim 2022; M. Bin Park et al. 2019). Luo et al (2019) described that HCl gas was released from fine particles due to strong solar irradiation in summer and the concentration of particulate Cl^- in winter showed a peak at 0.43 µm - 0.65 µm. These results support this study which shows that the fractional contribution of incinerator source was higher during SMP than during Non-SMP and higher in $PM_{1.0}$ than in $PM_{2.5}$. The CBPF plot shows mainly the southwest direction where incinerators in Gyeonggido including Anyang, Gwacheon, and Gunpo are located (J. Park et al. 2022).

Soil source was identified by high loadings and narrow DISP intervals of Mg, Al, Si, Ca, Ti, and Fe which were known as crustal elements (F. Yang et al. 2005; J. H. Lee and Hopke 2006). The average contributions of this source in $PM_{2.5}$ and $PM_{1.0}$ were 0.61 $\mu g/m^3$ (2.9%) and 0.30 $\mu g/m^3$ (1.9%), respectively. Particles emitted from mechanical or natural processes are known to have a high large particle fraction (Khan et al. 2021; J. B. Heo, Hopke, and Yi 2009; Miller-Schulze et al. 2015). Thus, the fractional contribution of soil source was higher in $PM_{2.5}$ than in $PM_{1.0}$. Since no Asian dust storms were observed during the sampling period, there was no significant seasonal pattern in the contribution and other characteristics were not found in the CBPF plot.

Industry source was identified by high loadings and narrow DISP intervals of Cr, Mn, Fe, Cu, and Zn which were mainly emitted from steel industries (Taiwo et al. 2014; Sylvestre et al. 2017). The average contributions of industry source in $PM_{2.5}$ and $PM_{1.0}$ were 1.65 $\mu g/m^3$ (7.8%) and 0.40 $\mu g/m^3$ (2.5%), respectively. According to Taiwo et al (2014), coarse particles were dominant in the industrial area compared to the background urban area, and the concentration of constituents used as markers of industry source showed peaks at not only less than 1 μm but also larger than 1 μm in the particle size distribution. This result supports that the fractional contribution of industry source is higher in $PM_{2.5}$ than in $PM_{1.0}$ like this study. In the CBPF plot of industry source, the value is high when the wind speed is low. This represents the characteristic of the local source. the plot shows that the direction of sources is mainly the south and west. The Sihwa and Banwol industrial complexes are located in the south of Seoul. In these industrial complexes, Fe from the steel industry, Zn and Pb from the nonferrous industry, and Cr from the plating industry are emitted (Kang et al. 2018). In addition, many industrial complexes are located in Incheon in the west.

Coal combustion source was identified by high loadings and narrow DISP intervals of As and Pb. The average contributions of this source in $PM_{2.5}$ and $PM_{1.0}$ were 1.77 $\mu g/m^3$ (8.4%) and 1.22 $\mu g/m^3$ (7.6%), respectively. As and Pb were mainly emitted from coal combustion processes such as coal-fired power plants, and the

concentration of these constituents is high in the accumulation mode (Zhu et al. 2016; J. Duan et al. 2012). Coal combustion source increased significantly during SMP. This is known as the influence of increased fuel use for heating in winter (E. H. Park et al. 2020; M. Bin Park et al. 2019). The CBPF plot mainly indicates the northwest direction, and in the case of $PM_{1.0}$, it also indicates the southwest direction. In the northwest of Seoul, many industrial complexes are located in Incheon and Gimpo. In addition, M. Bin Park et al (2019) described that there might be an influence of coal-burning activities in North Korea. For the southwest, coal-fired plants are located in Dangjin and Yeongheung.

Oil combustion source accounted for 0.40 $\mu g/m^3$ (1.9%) and 0.35 $\mu g/m^3$ (2.2%) in $PM_{2.5}$ and $PM_{1.0}$, respectively. V and Ni had high loadings and narrow DISP intervals. V and Ni are mainly emitted from crude oil combustion and ship emission (Viana et al. 2008; Pey et al. 2013).

Aged sea salt source was identified by high loading and narrow DISP interval of Na^+. The average contributions of this source in $PM_{2.5}$ and $PM_{1.0}$ were 0.72 $\mu g/m^3$ (3.4%) and 0.64 $\mu g/m^3$ (4.0%), respectively. It is mainly produced by the reaction of sea salt particles from the sea with SO_2 in the atmosphere. Thus, it was likely to be influenced by anthropogenic sources such as ship emissions (Waked et al. 2014; S. Kim et al. 2018). In the CBPF plot of oil combustion source and aged sea salt source, they show mainly the west coast of Seoul.

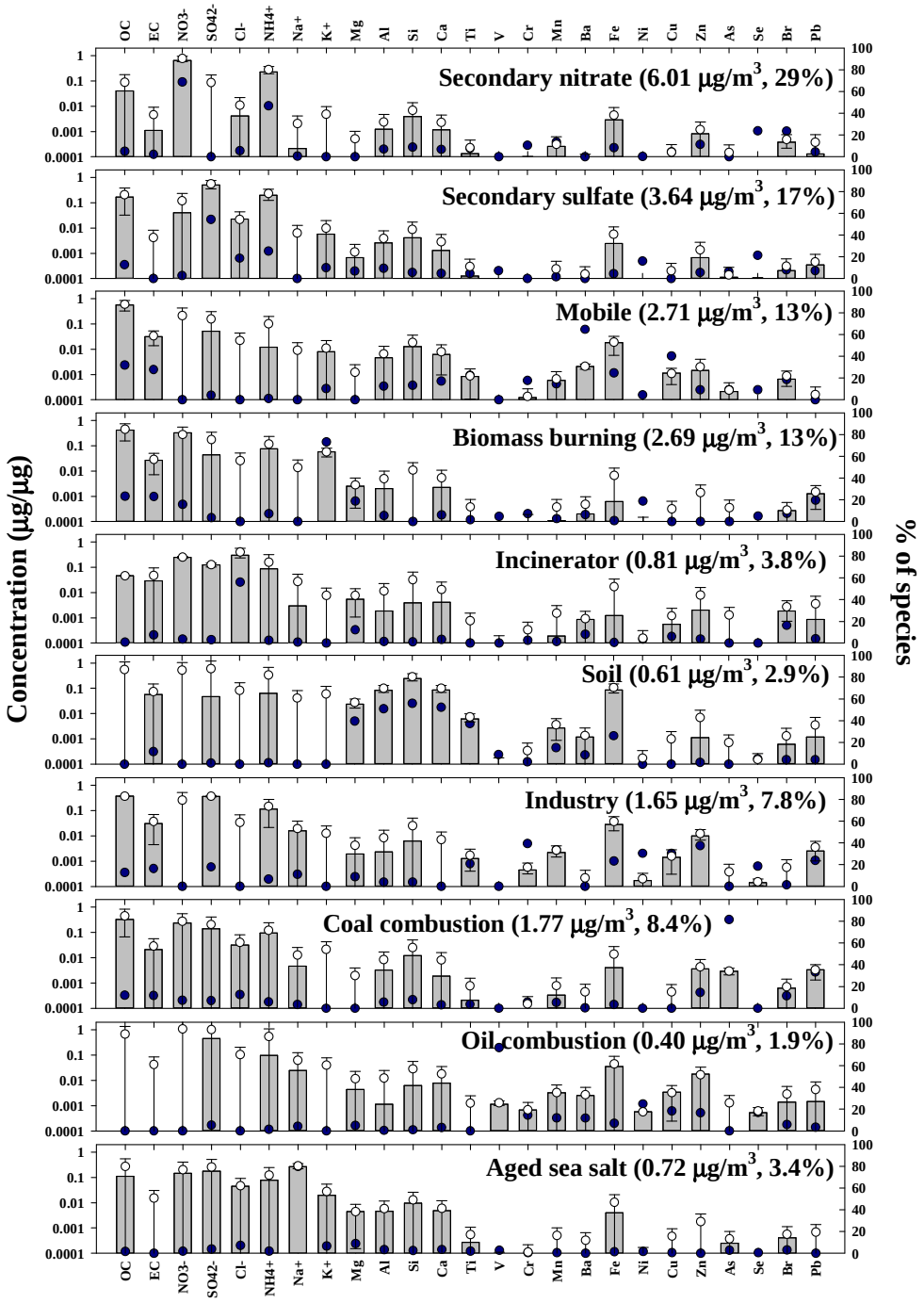

Figure 4 Source profiles of $PM_{2.5}$ in Seoul from June 2021 to February 2022

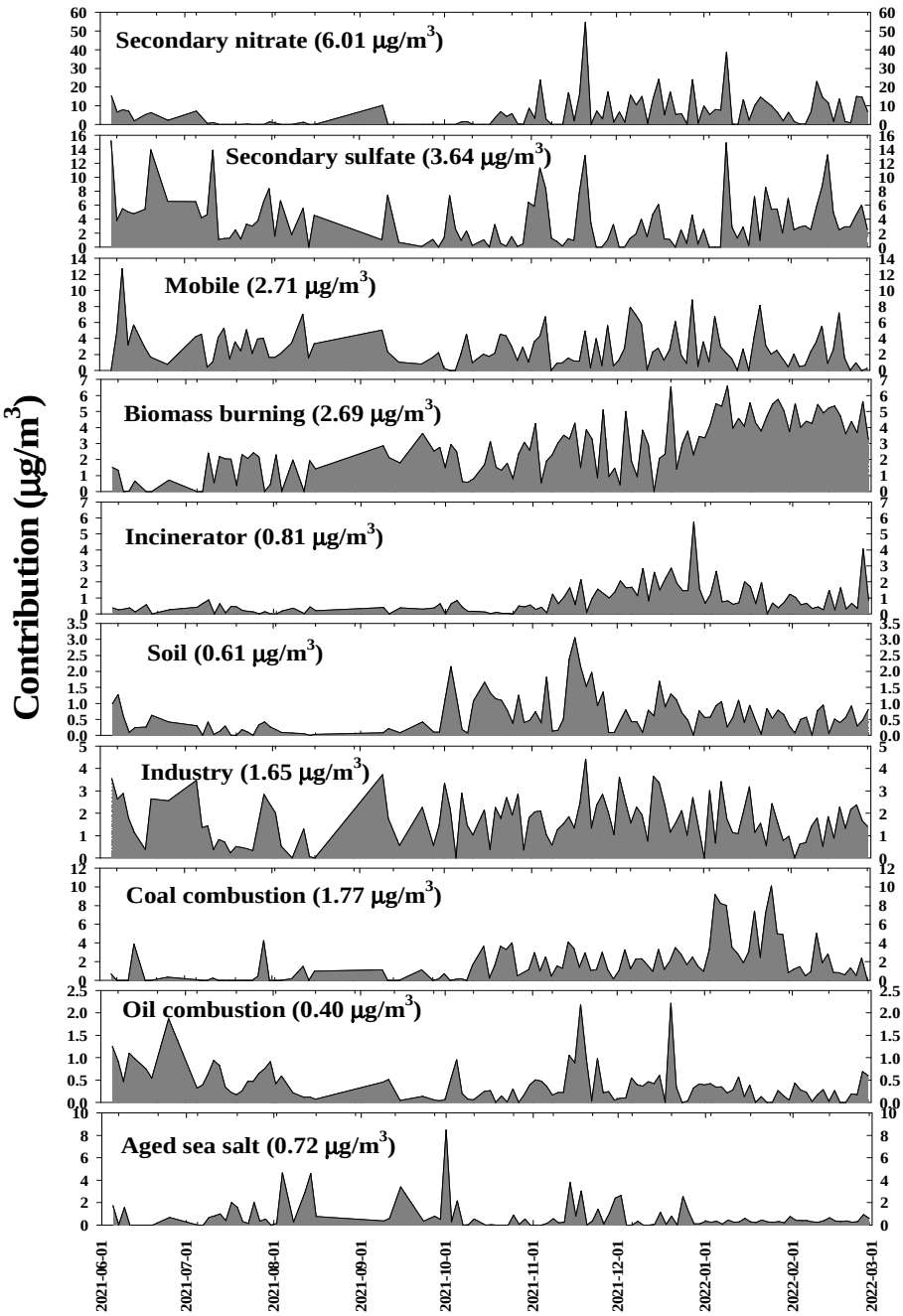

Figure 5 PMF source contribution of $PM_{2.5}$ in Seoul from June 2021 to February 2022

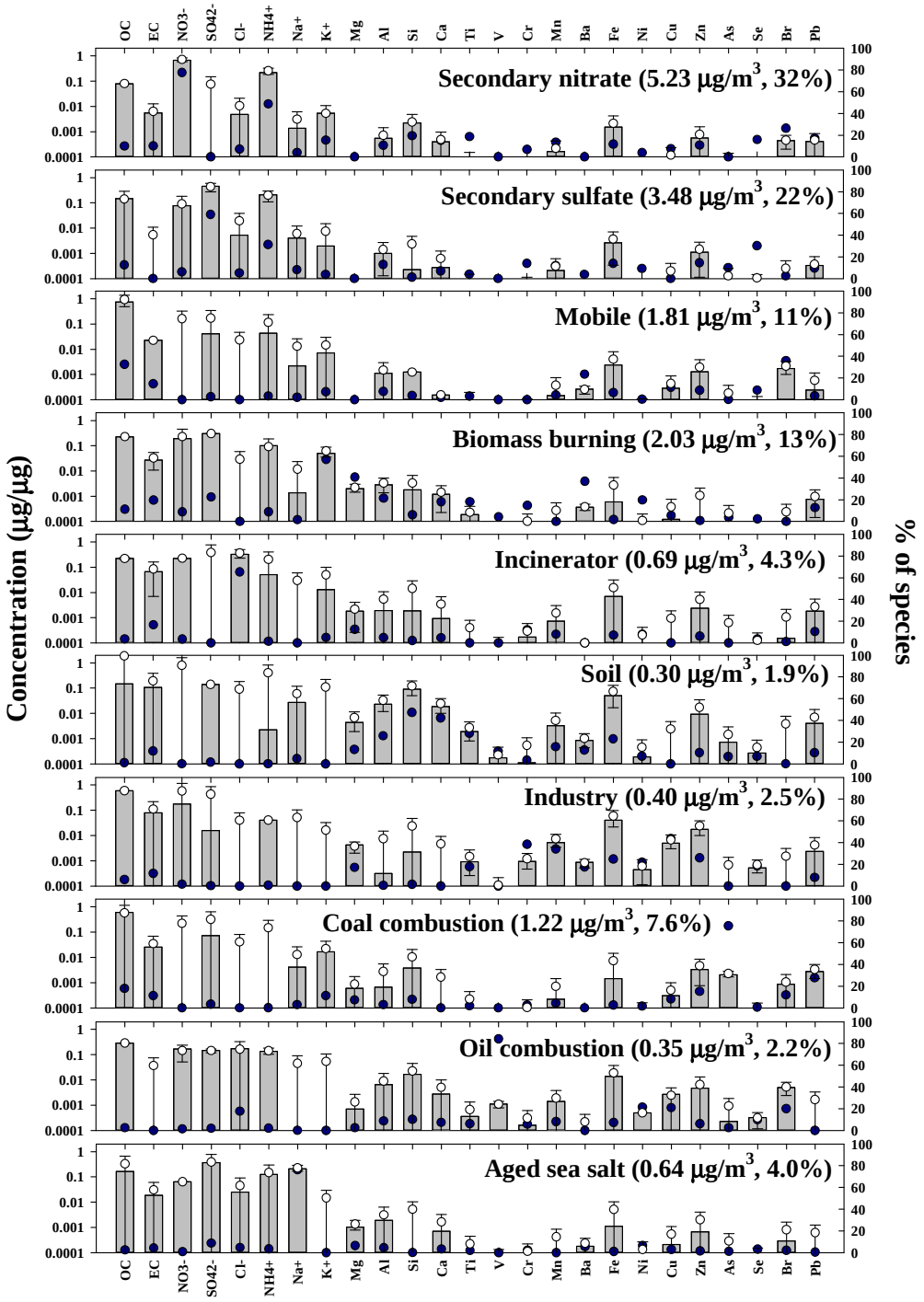

Figure 6 Source profiles of $PM_{1.0}$ in Seoul from June 2021 to February 2022

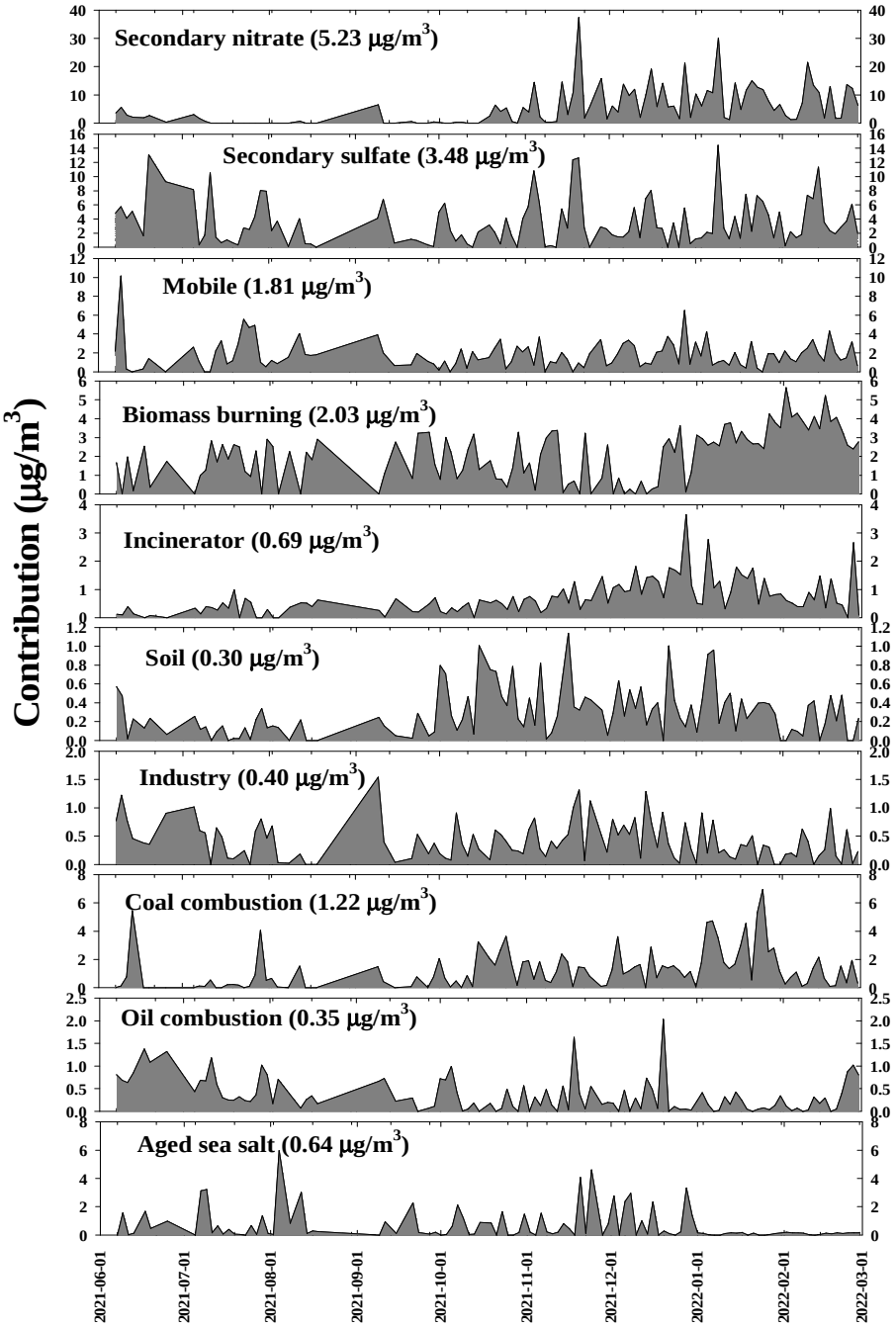

Figure 7 PMF source contribution of $PM_{1.0}$ in Seoul from June 2021 to February 2022

Table 2 Comparison of the source contribution during SMP (2021.12.-2022.02.) with during Non-SMP (2021.06.-2021.11.) (yellow boxes indicate '$p < 0.01$' on the t-test).

	$PM_{2.5}$				$PM_{1.0}$			
	Non-SMP		SMP		Non-SMP		SMP	
	$\mu g/m^3$	%	$\mu g/m^3$	%	$\mu g/m^3$	%	$\mu g/m^3$	%
Secondary nitrate	3.97	23%	9.17	34%	2.64	21%	8.97	42%
Secondary sulfate	3.76	22%	3.63	14%	3.39	27%	3.60	17%
Mobile	2.70	16%	2.72	10%	1.74	14%	1.91	9.0%
Biomass burning	1.79	10%	4.00	15%	1.63	13%	2.61	12%
Incinerator	0.43	2.5%	1.35	5.1%	0.40	3.2%	1.10	5.2%
Soil	0.61	3.6%	0.61	2.3%	0.29	2.3%	0.32	1.5%
Industry	1.61	9.3%	1.69	6.3%	0.43	3.4%	0.37	1.7%
Coal combustion	1.00	5.8%	2.88	11%	0.86	6.8%	1.74	8.2%
Oil combustion	0.48	2.8%	0.30	1.1%	0.43	3.4%	0.25	1.2%
Aged sea salt	0.92	5.3%	0.44	1.6%	0.78	6.2%	0.44	2.0%

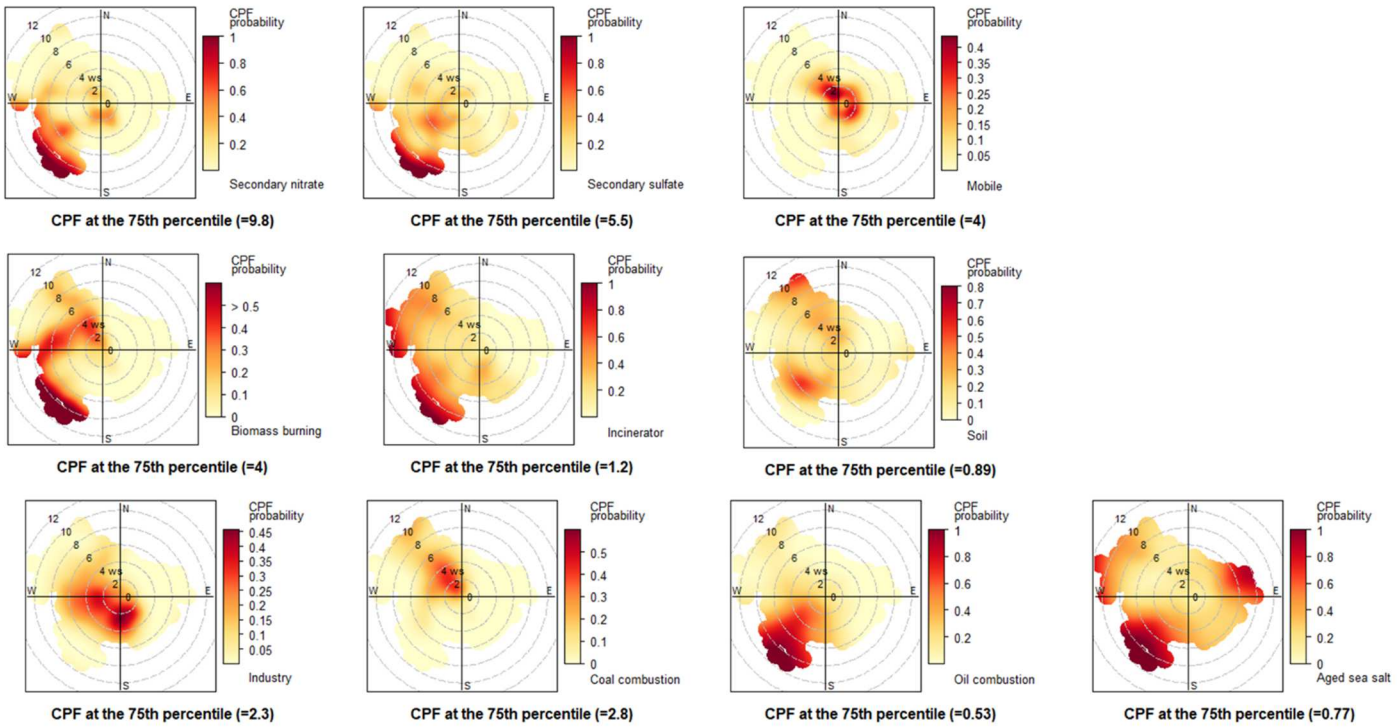

Figure 8 CBPF plots of $PM_{2.5}$ sources (From the top left to the bottom right : Secondary nitrate, Secondary sulfate, Mobile, Biomass burning, Incinerator, Soil, Industry, Coal combustion, Oil combustion, and Aged sea salt)

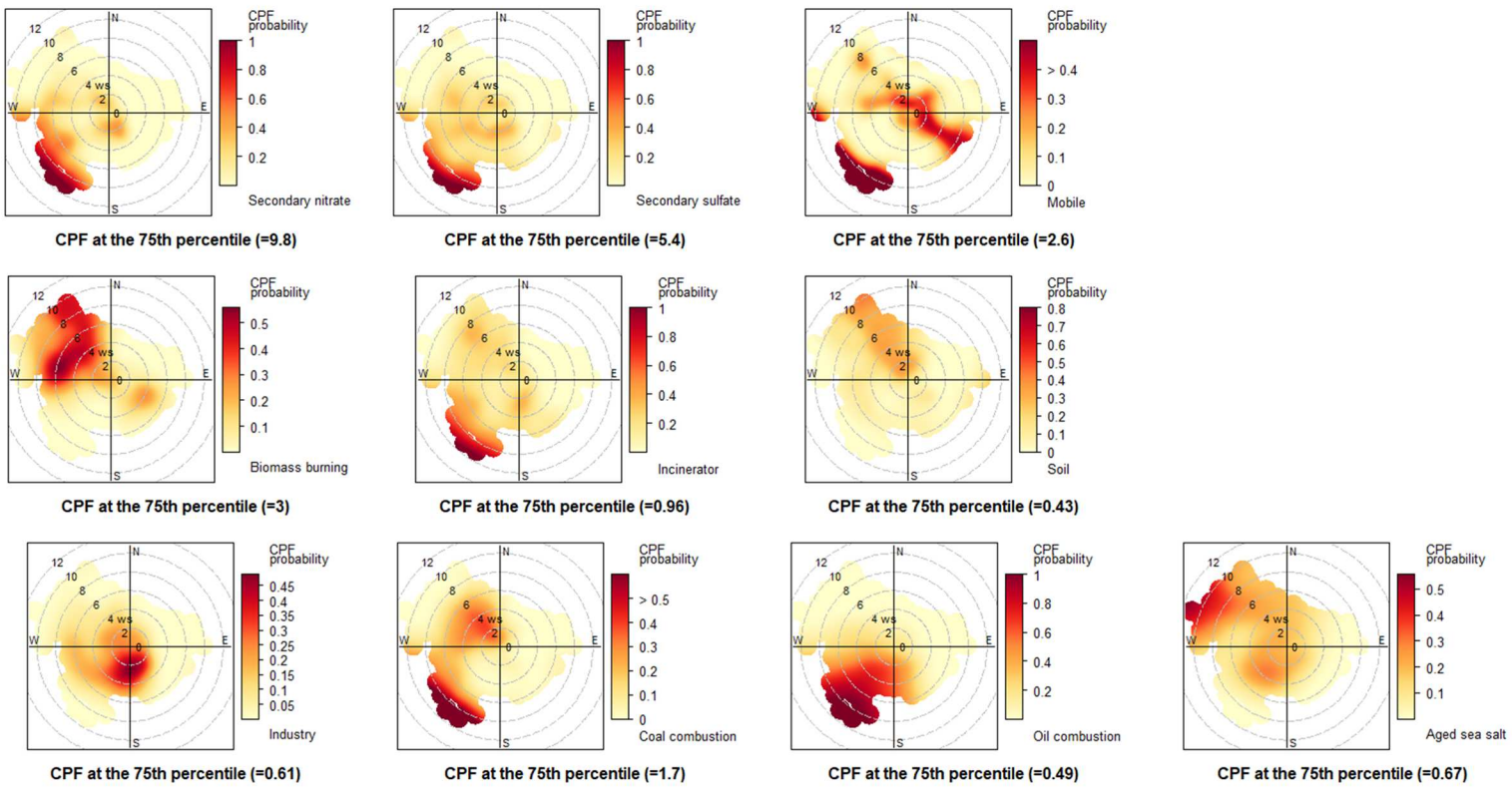

Figure 9 CBPF plots of $PM_{1.0}$ sources (From the top left to the bottom right : Secondary nitrate, Secondary sulfate, Mobile, Biomass burning, Incinerator, Soil, Industry, Coal combustion, Oil combustion, and Aged sea salt)

3.3 Cluster analysis

From the cluster analysis using the HYSPLIT 4 model, a total of six clusters were classified from C1 to C6. The number of clusters was determined based on spatial variance according to guidelines of NOAA.

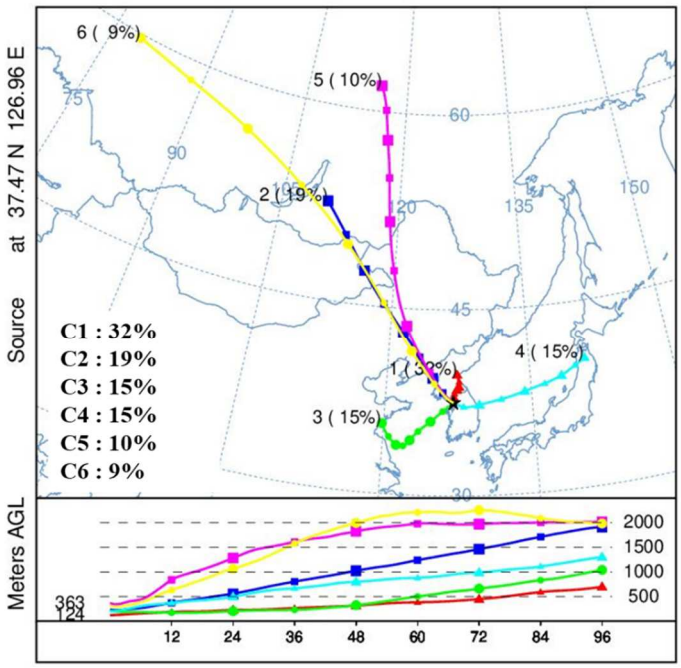

Figure 10 Mean 96 h backward trajectory cluster arriving at Seoul from June 2021 to February 2022

C1 was a case of staying in Korea because the wind speed was not strong, and it corresponded to 32% of the total period. The average mass concentrations of $PM_{2.5}$ and $PM_{1.0}$ were 20.9 μg/m^3 and 16.1 μg/m^3, respectively.

C2, C5, and C6 all showed the influence of strong winter monsoons. They showed inflows through China and North Korea from Mongolia and Siberia. Since these three clusters flow in a similar pathway, they were grouped into one group to compare the clusters. This group accounted for 38% of the total period, and the average mass concentrations of $PM_{2.5}$ and $PM_{1.0}$ were 19.9 μg/m^3 and 15.2 μg/m^3,

respectively, which were similar to those of C1. In this group, the average contribution of biomass burning source was higher than other clusters. In North Korea, biomass is used as a residential fuel, and Manchuria, China was indicated as potential sources of transported biomass burning in other studies (B. M. Kim et al. 2016; I. S. Kim, Lee, and Kim 2013).

C3 showed the inflow from Shandong province in China, accounting for 15% of the total period. For C3, the average mass concentrations of $PM_{2.5}$ and $PM_{1.0}$ were 28.7 $\mu g/m^3$ and 19.8 $\mu g/m^3$, respectively, the highest among the clusters. In addition, the average contributions of secondary nitrate, secondary sulfate, and oil combustion sources were higher than other clusters. As secondary nitrate and secondary sulfate sources are secondary aerosol, it is likely to be influenced by long-range transport (B. M. Kim et al. 2016). In addition, Shandong province is known to have high NO_X and SO_2 emissions (Junfeng Wang et al. 2018; Zhao et al. 2015). In the case of oil combustion source, it seemed to be influenced by many ships on the west coast of Korea.

C4 showed the influence of the summer monsoon and accounted for 15% of the total period. The average mass concentrations of $PM_{2.5}$ and $PM_{1.0}$ were 13.2 $\mu g/m^3$ and 9.3 $\mu g/m^3$, respectively, the lowest among the clusters.

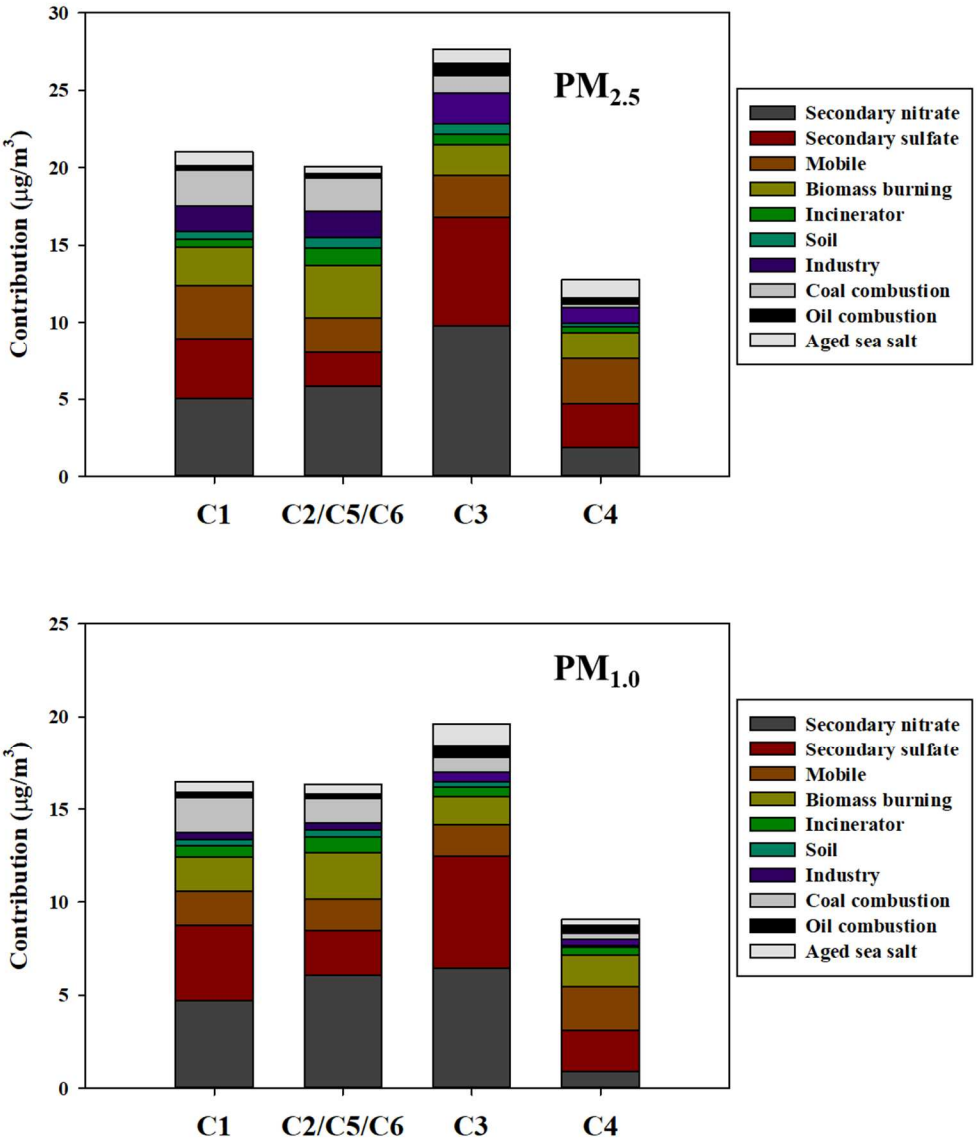

Figure 11 Source contribution of each cluster

3.4 PSCF of secondary sources

Secondary sources (secondary nitrate and secondary sulfate sources) in Seoul are known as sources that are influenced by long-range transport (B. M. Kim et al. 2016). In the cluster analysis of this study, it was indicated that the contributions of secondary sources were higher in the case of the inflow from foreign regions than stagnation. Thus, the PSCF was performed to understand the potential source area of secondary sources.

To compare the possible areas of potential source of $PM_{2.5-1.0}$ and $PM_{1.0}$, the contribution of $PM_{2.5-1.0}$ was calculated by subtracting the contribution of $PM_{1.0}$ from the contribution of $PM_{2.5}$. PSCF results were divided into SMP and Non-SMP for comparison according to season and were shown in Figure 12 ~ Figure 15.

In the case of secondary nitrate source of $PM_{2.5-1.0}$ and $PM_{1.0}$ during SMP, Jing-Jin-Ji region (Beijing, Tianjin, and Hebei province), Shandong province, and Henan province were indicated as possible source areas. For $PM_{1.0}$, these regions showed a high PSCF value but showed a low PSCF value in Jiangsu province and Inner Mongolia, where the $PM_{1.0}/PM_{2.5}$ ratio was not high in previous study (G. Chen et al. 2018). $PM_{2.5-1.0}$ indicated a wider area as a possible source area, but the upper 25% value was low. These regions, known as the North China Plain, are the densely populated and industrialized regions of China (L. Wang et al. 2018; Junfeng Wang et al. 2018; Zhao et al. 2015; Hu et al. 2014; B. M. Kim et al. 2016). In Hu et al (2014), the average mass concentration of $PM_{2.5}$ in these regions exceeded the World Health Organization guideline value. In addition, since from November to March in these regions is the heating season, SO_2 and NO_2 emissions are known to increase during this season (Pang et al. 2020; Meng et al. 2018).

For Non-SMP, in $PM_{1.0}$, Shandong province and the surrounding sea were mainly indicated as possible source areas. For $PM_{2.5-1.0}$, the Yellow Sea was indicated. The high concentration of NH_3 emitted from Shandong province was likely to influence the secondary nitrate formation, and there might be the influence of NO_X emitted from ship calls in the sea which increase during Non-SMP (Wen et al. 2015; Nunes

et al. 2017).

For secondary sulfate source of $PM_{2.5-1.0}$ during SMP, Mongolia was indicated as a possible source area. Mongolia is a region that uses a lot of coal for heating in traditional dwellings during winter (Warburton et al. 2018; Batmunkh et al. 2013). In the case of $PM_{1.0}$ during SMP, areas similar to those of secondary nitrate source were indicated as possible source areas. It indicated that secondary sulfate from North China Plain contributed to $PM_{1.0}$ in Seoul during SMP. For Non-SMP, the Yellow Sea was the main possible source area in $PM_{1.0}$, and $PM_{2.5-1.0}$ mainly indicated the southern coast of Korea. They were likely to be influenced from ship emissions.

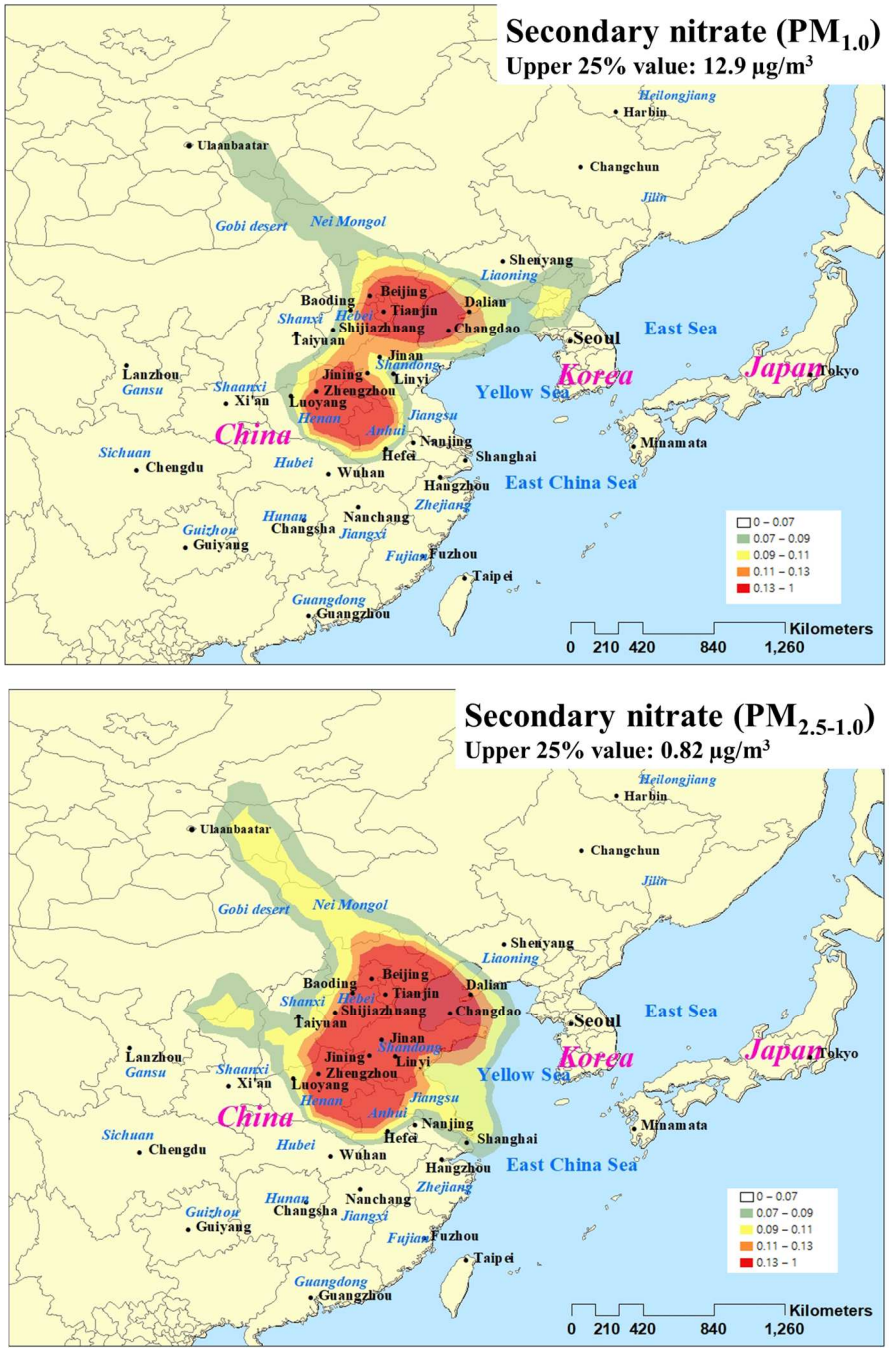

Figure 12 PSCF maps of secondary nitrate during SMP (2021.12.-2022.02.)

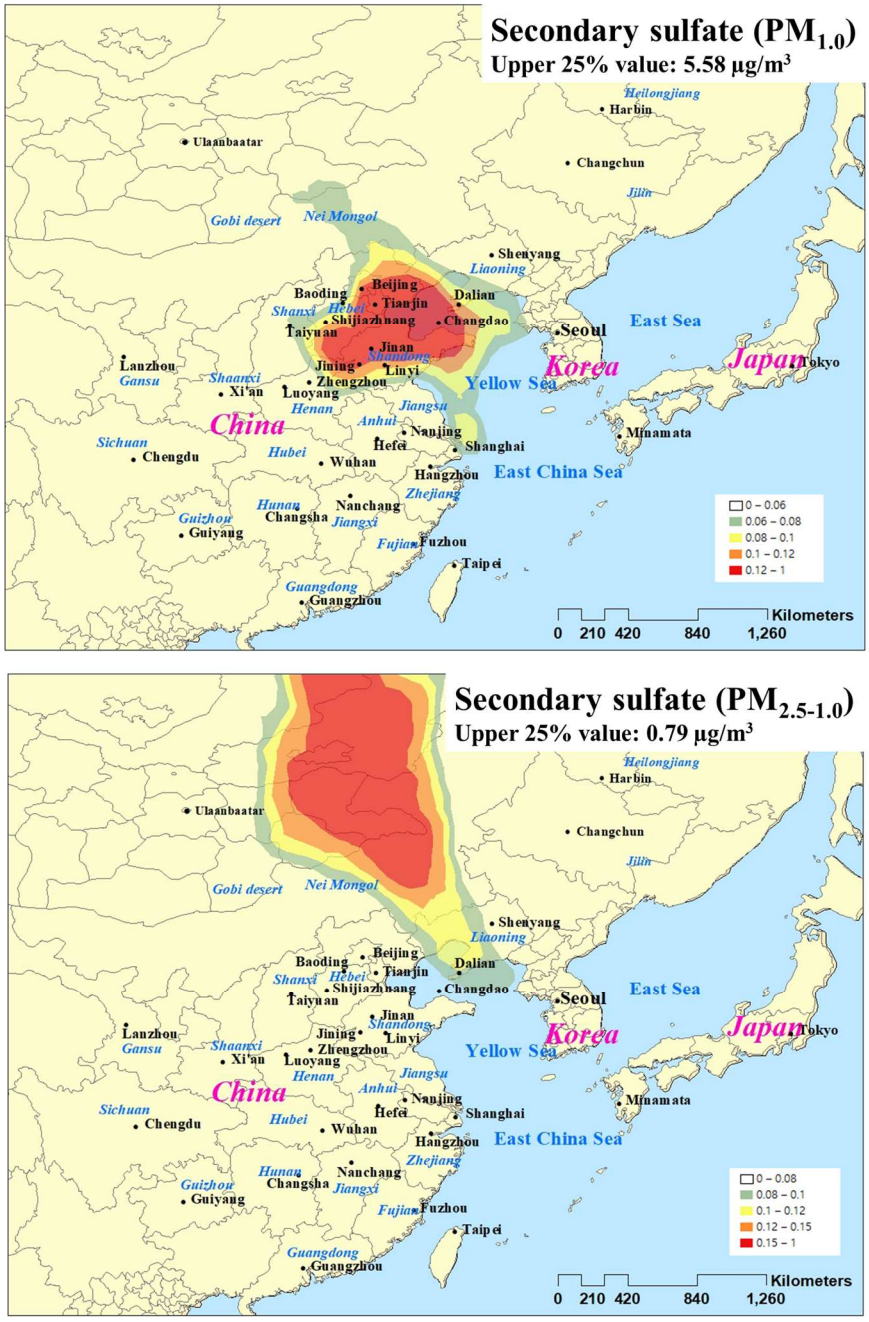

Figure 13 PSCF maps of secondary sulfate during SMP (2021.12.-2022.02.)

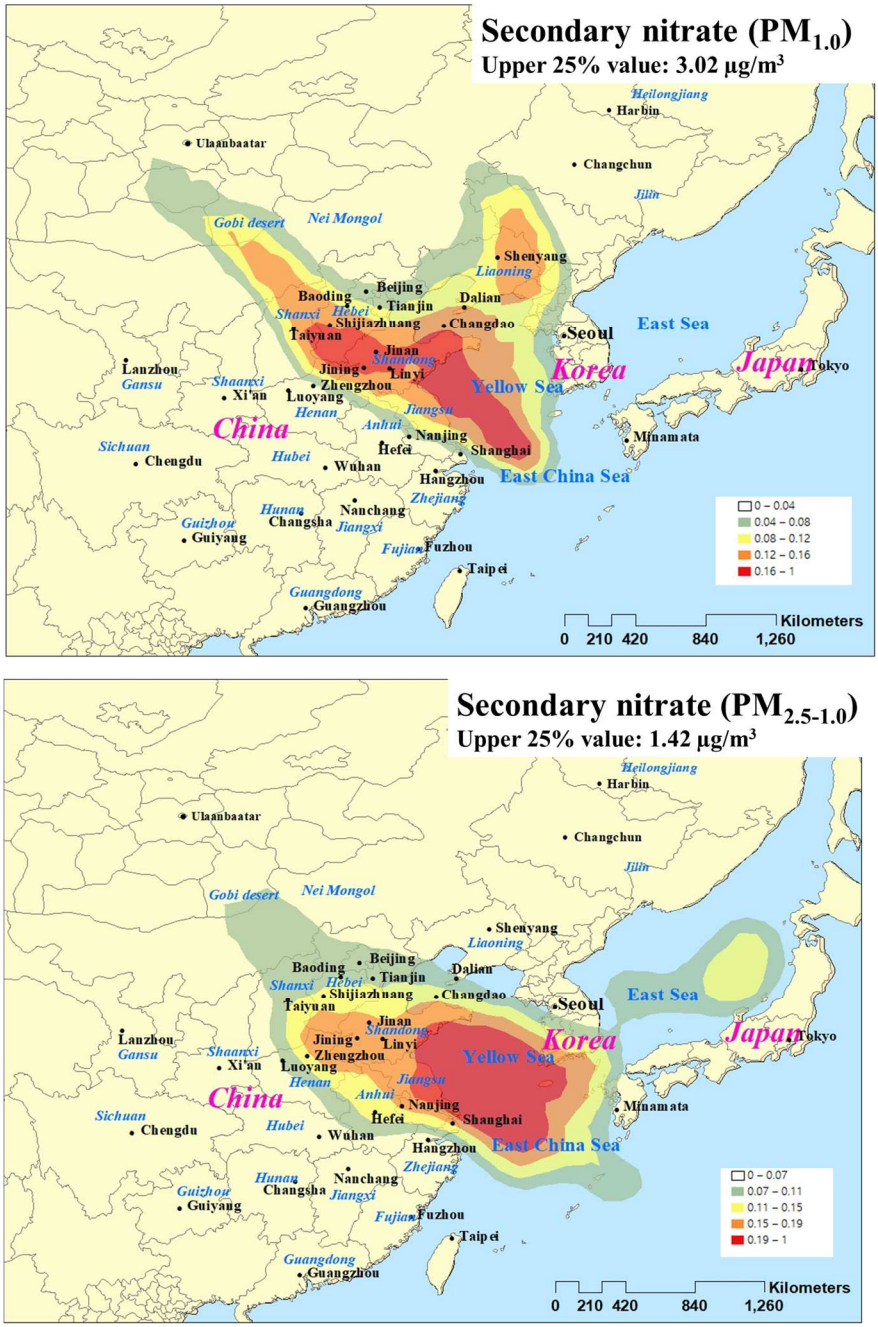

Figure 14 PSCF maps of secondary nitrate during Non-SMP (2021.06.-2021.11.)

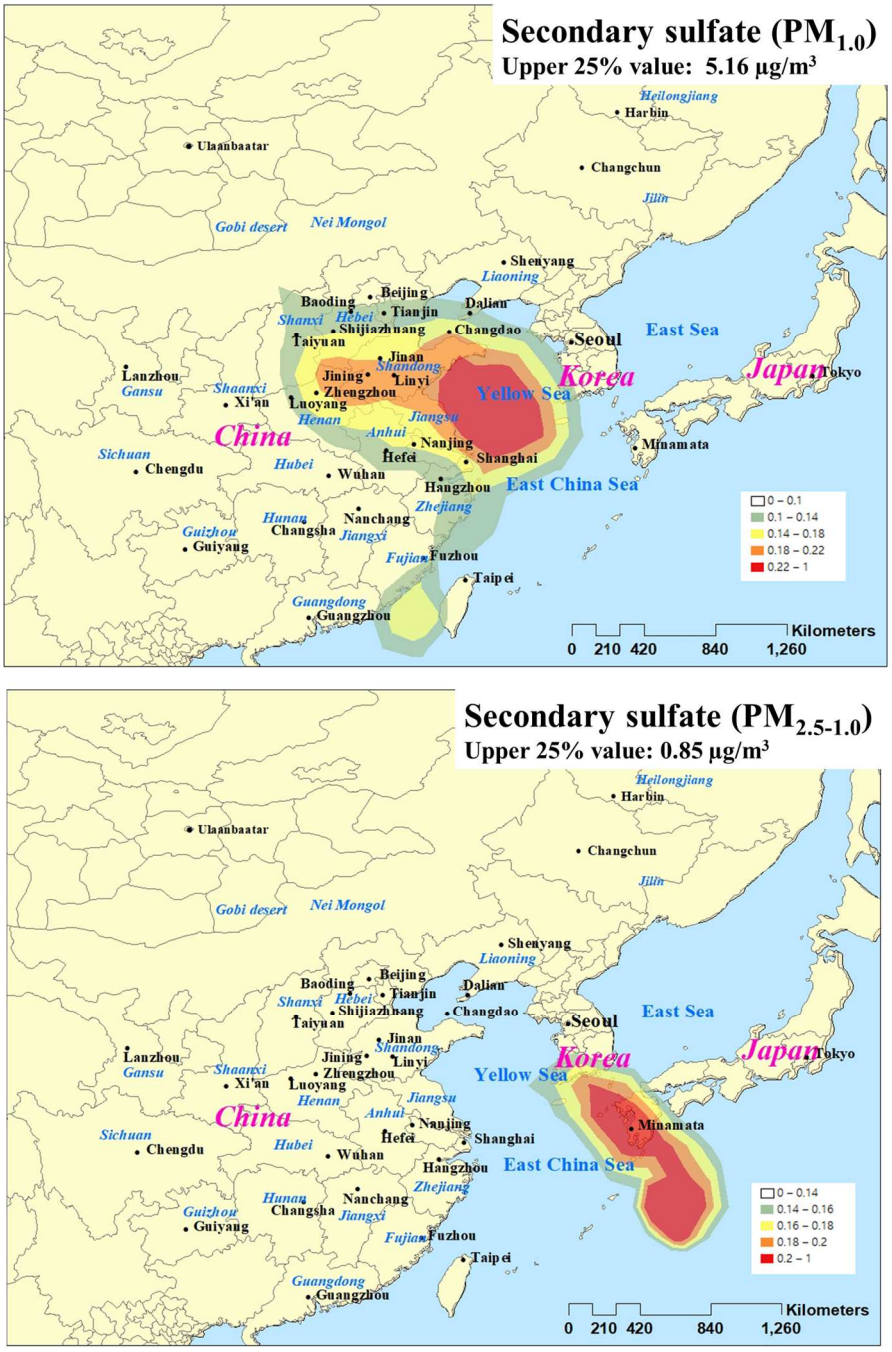

Figure 15 PSCF maps of secondary sulfate during Non-SMP (2021.06.-2021.11.)

3.5 High concentration events (HCEs)

The Mann Whitney U test was used to verify whether the change in the source contribution was significant when high concentration events (HCEs) of $PM_{2.5}$ occurred ($P<0.01$).

In the case of $PM_{2.5}$, secondary nitrate, secondary sulfate, biomass burning, and coal combustion significantly increased, and for $PM_{1.0}$, secondary nitrate, secondary sulfate, incinerator, and coal combustion significantly increased. In order to understand the influence of $PM_{1.0}$ on common sources with significant increase in $PM_{2.5}$ and $PM_{1.0}$, the contribution of $PM_{2.5-1.0}$ was used. $PM_{2.5-1.0}$ increased significantly in secondary nitrate and coal combustion but not in secondary sulfate. Thus, the significant increase in the contribution of secondary sulfate source in HCEs of $PM_{2.5}$ was shown to be influenced by the increase in $PM_{1.0}$.

Since secondary sources are influenced by long-range transport, the significant increase in HCEs also was influenced by long-range transport. In particular, in this study, HCEs except one day occurred between November and February, when most of the days correspond to the seasonal management period. Thus, significant increase in the contribution of secondary nitrate in HCEs was likely to be influenced from North China Plain, which was a possible source area of secondary nitrate during SMP as shown in the PSCF results. This influence from North China Plain was important considering that from November to February corresponded to the heating season of North China and all days flowing from Shandong province (C3 in the cluster analysis) during the heating season were verified as HCEs.

In the case of secondary sulfate, only in $PM_{1.0}$ the contribution significantly increased and North China Plain was indicated as a possible source area during SMP. Thus, the significant increase in the contribution of secondary sulfate in $PM_{2.5}$ when HCEs occurred was Influenced by significant increase in $PM_{1.0}$, which was likely to be emitted from North China Plain. In addition, since secondary formation of sulfate is active in summer, the increase in sulfate during winter is known to be influenced by heating and cooking using coal (Dai et al. 2018). Since coal is rarely used for

heating and cooking in South Korea, the foreign influences that contribute to significant increase in secondary sulfate when HCEs occur during winter need to be considered more important than for secondary nitrate (M. Bin Park et al. 2019). In addition, there was no large difference in $PM_{1.0}/PM_{2.5}$ ratios of mass concentration between Non-HCEs (0.75) and HCEs (0.71). Also, there was no difference in $PM_{1.0}/PM_{2.5}$ ratios (source contribution) of secondary nitrate (Non-HCEs: 0.86, HCEs: 0.85), but for secondary sulfate (Non-HCEs: 0.78, HCEs: 0.96), the ratio of $PM_{1.0}$ increased in HCEs. This also indicated that the influence of $PM_{1.0}$ was important in secondary sulfate when HCEs occurred.

In the case of biomass burning that increased significantly only in $PM_{2.5}$ when HCEs occurred, the contribution of biomass burning significantly increased in $PM_{2.5-1.0}$. The CBPF plot of $PM_{2.5}$ in biomass burning showed the southwest when the wind speed was strong, which was similar to secondary sources. It was likely to be influenced from distant sources. The PSCF of biomass burning in $PM_{2.5-1.0}$ showed North China Plain as a possible source area (Figure S3). Thus, like secondary sources, it seemed that this region influenced the significant increase in the contribution of biomass burning when HCEs occurred. From these results, transported biomass burning unlike secondary sulfate was likely to contribute importantly to $PM_{2.5-1.0}$. However, there might be an influence of the coagulation of particles during the transport process (Sakamoto et al. 2016).

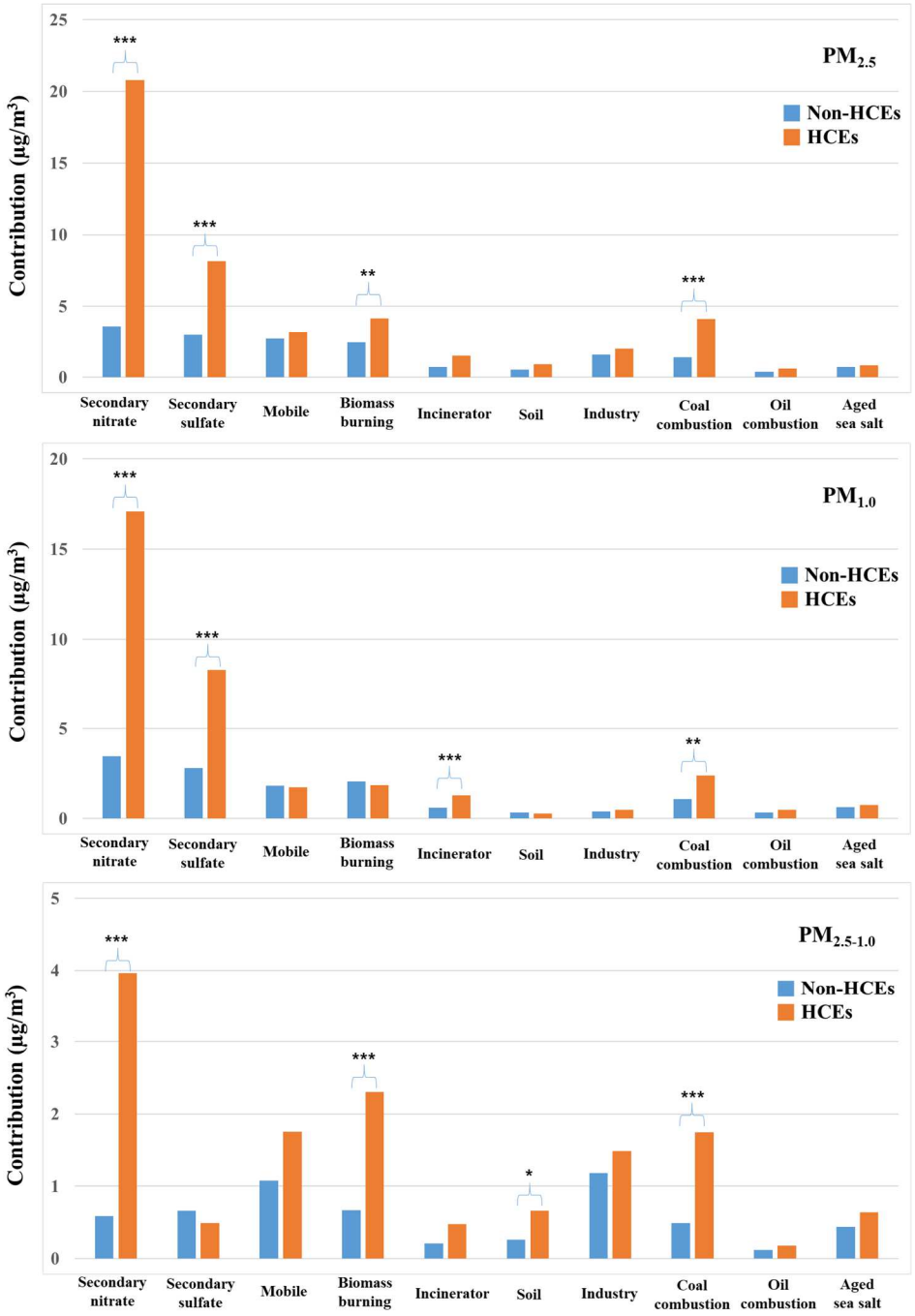

Figure 16 The source contributions in HCEs and Non-HCEs (***: P<0.001, **: P<0.01, *: P<0.05)

3.6 DTT assay

45 high-volume samples during the seasonal management period (from December 2021 to February 2022) were used for the DTT assay. The average DTTv of $PM_{2.5}$ was 0.611 nmol/min/m^3, and the average DTTv of $PM_{1.0}$ was 0.588 nmol/min/m^3, which showed that the oxidative potential of $PM_{2.5}$ was higher than $PM_{1.0}$. However, the values calculated from dividing each DTTv by the mass concentration were 0.027 nmol/min/μg in $PM_{2.5}$ and 0.035 nmol/min/μg in $PM_{1.0}$, which indicated that the value of $PM_{1.0}$ was higher. In a study measuring the oxidative potential of $PM_{2.5}$ during winter in Gwangju as the same method, its average value was 0.62 nmol/min/m^3 which was similar to this study (B. J. Lee et al. 2020). The DTTv of $PM_{1.0}$ / DTTv of $PM_{2.5}$ ratio was 0.955, which was higher than the ratio of mass concentration (0.778) during the same period. Thus, it indicated that most of the oxidative potential of $PM_{2.5}$ was the influence from $PM_{1.0}$.

Table 3 shows results of Pearson correlation analysis between DTTv and concentrations of chemical constituents. The mass concentration had a high positive correlation with DTTv ($PM_{2.5}$: r=0.847, $PM_{1.0}$: r=0.661). For both $PM_{2.5}$ and $PM_{1.0}$, OC had the highest correlation with DTTv ($PM_{2.5}$: r=0.873, $PM_{1.0}$: r=0.786), and in common, NO_3^-, NH_4^+, Mn, Fe, Zn, and Pb had high correlation. Many studies showed that OC and metals were representative constituents that cause oxidative potential (Saffari et al. 2014; H. Yu et al. 2018; Feng et al. 2022; Verma et al. 2015; MacIejczyk et al. 2010). For NO_3^- and NH_4^+, this might be because winter samples were used for DTT assay. During winter, secondary nitrate formation occurs actively contributing greatly to particulate matter as shown in PMF result of this study. In addition, other studies with similar results suggested that there were influences of constituents related to secondary aerosol formation (Jingpeng Wang et al. 2019; Ma et al. 2018). In particular, some studies showed the significance of nitrate in SOA (secondary organic aerosol) formation and showed that SOA produced under high-NO_X condition than low-NO_X condition had a high oxidative potential (Kramer et al. 2016; Mabato et al. 2022). SOA is well known as a constituent related to oxidative potential (Jiang et al. 2019).

Multiple linear regression was used to compare the influence of each source on the oxidative potential of $PM_{2.5}$ and $PM_{1.0}$. The DTTv was used as the dependent variable and the contributions of sources were used as the independent variable. In addition, variables were selected by the backward elimination method (Ryu, Kim, and Kang 2016). Durbin-Watson value and Variance Inflation Factor were used to verify autocorrelation and multicollinearity (Table S2 and Table S3).

In $PM_{2.5}$, secondary nitrate, biomass burning, industry, and coal combustion sources were selected as variables that represented DTTv ($P<0.05$), and the F-test result of this model was significant ($P<0.01$). The adjusted R^2 was 0.76, which showed that the regression equation represented the dependent variable well. For $PM_{1.0}$, secondary nitrate, biomass burning, incinerator, and soil sources were selected as variables ($P<0.05$). The adjusted R^2 was 0.51, which was lower than that of $PM_{2.5}$, but the model was significant in the F-test ($P<0.01$).

In both $PM_{2.5}$ and $PM_{1.0}$, secondary nitrate and biomass burning were selected to be variables that represented DTTv. OC, which was one of the main marker constituents of biomass burning, had a high correlation with DTTv. In addition, it is known that the humic-like substances which are abundantly emitted from biomass burning contribute to oxidative potential (Verma et al. 2015; Ma et al. 2018). Thus, biomass burning was an important source influencing oxidative potential in Seoul.

For secondary nitrate, NO_3^- and NH_4^+, the main marker constituents of this source, had a high correlation with DTTv. As mentioned above, this source in multiple linear regression was likely to represent influences related to secondary formation process and seasonal characteristic of constituents (NO_3^- and NH_4^+) rather than a direct influence on oxidative potential.

In $PM_{2.5}$, coal combustion and industry were also selected. It is known that Pb emitted from coal combustion and metals (Fe, Mn, Zn and Cr) from industry influence DTT (S. Y. Yu et al. 2019; Feng et al. 2022). These constituents also had a high correlation with DTTv in this study.

Soil and incinerator were selected as variables in $PM_{1.0}$, there seemed to be the influence of metals included in soil source (Bates et al. 2019). In the case of incinerator source, there seemed to be the influence of OC, Zn, and Pb emitted from Incineration (Pan et al. 2013). The difference between $PM_{2.5}$ and $PM_{1.0}$ in some variables representing DTTv was likely to occur because concentrations of trace elements influencing oxidative potential were relatively low in $PM_{1.0}$.

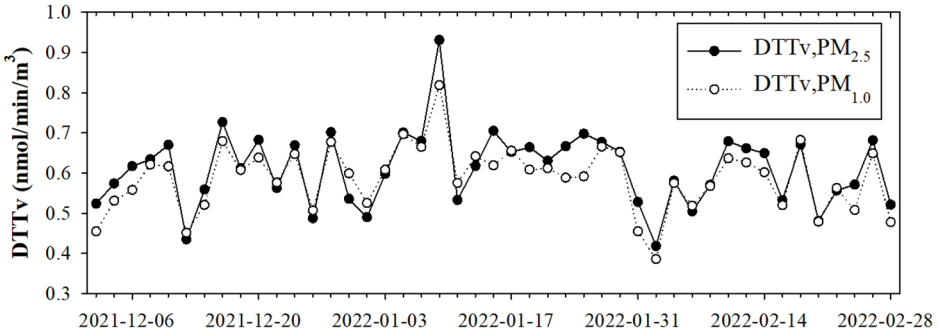

Figure 17 Time series of DTTv from December 2021 to February 2022

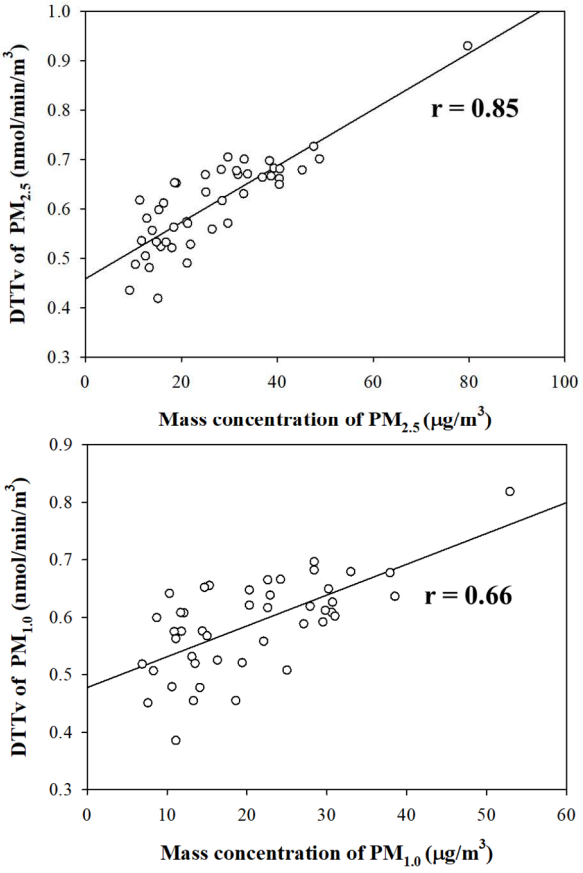

Figure 18 Scatterplots of mass concentration and DTTv

Table 3 Correlation coefficients between constituents and DTTv according to Pearson correlation analysis (**: P<0.01, *:P<0.05)

	Correlation coefficient ($PM_{2.5}$)	**Correlation coefficient ($PM_{1.0}$)**
Mass concentration	**0.847****	**0.661****
OC	**0.873****	**0.786****
EC	0.554**	0.582**
NO_3^-	**0.790****	**0.608****
SO_4^{2-}	0.664**	0.438**
Cl^-	0.536**	0.489**
NH_4^+	**0.792****	**0.601****
Na^+	0.106	0.071
K^+	0.574**	0.437**
Mg	0.262	0.123
Al	0.652**	0.550**
Si	0.645**	0.538**
Ca	0.555**	0.595**
Ti	0.608**	0.472**
V	0.127	0.011
Cr	**0.716****	0.558**
Mn	**0.793****	**0.630****
Ba	0.176	-0.171
Fe	**0.761****	**0.668****
Ni	0.461**	0.363*
Cu	0.484**	0.410**
Zn	**0.799****	**0.650****
As	0.574**	0.393**
Se	0.648**	0.526**
Br	0.619**	0.469**
Pb	**0.780****	**0.715****

4. Summary and Conclusion

In this study a total of 123 samples for each $PM_{2.5}$ and $PM_{1.0}$ in Seoul were analyzed, the average mass concentrations of $PM_{2.5}$ and $PM_{1.0}$ during the sampling period were 20.1 (± 14.1) $\mu g/m^3$ and 15.1 (± 10.2) $\mu g/m^3$, respectively. $PM_{1.0}$ accounted for about 75% of $PM_{2.5}$. This high $PM_{1.0}$ fraction indicated that secondary sources and combustion-related sources greatly contributed to $PM_{2.5}$ in Seoul. Most of OC, EC, NO_3^-, SO_4^{2-}, and NH_4^+ in $PM_{2.5}$ belonged to $PM_{1.0}$, and the OC, SO_4^{2-}, and NH_4^+ fractions in total concentration were significantly higher in $PM_{1.0}$ than in $PM_{2.5}$. The crustal elements fraction was significantly higher in $PM_{2.5}$ than in $PM_{1.0.}$

From the source apportionment by the PMF model, ten sources (Secondary nitrate, Secondary sulfate, Mobile, Biomass burning, Incinerator, Soil, Industry, Coal combustion, Oil combustion, and Aged sea salt) contributed to both $PM_{2.5}$ and $PM_{1.0}$. In common, secondary nitrate and secondary sulfate had high contribution, but the fractional contributions (%) of these sources were higher in $PM_{1.0}$. The fractional contribution of industry and soil sources in $PM_{2.5}$ was higher than in $PM_{1.0}$. From this, it was verified that secondary sources were important for $PM_{1.0}$ and the influence from natural and mechanical processes was large in $PM_{2.5}$. There were also differences in the constituents of sources. In particular, $PM_{1.0}$ from mobile source did not show high loadings of constituents emitted from road soil and brake lining. Thus, it was possible to observe the contribution of mobile exhaust gas excluding the influence of road dust from the research into $PM_{1.0}$ (Hien et al. 2021). In the CBPF plot, the main directions of local sources were well represented. Many sources of $PM_{2.5}$ and $PM_{1.0}$ in Seoul were likely to be influenced by the south and the west, where the Sihwa and Banwol industrial complexes, Gimpo industrial Complex, and Yeongdong Expressway are located.

In the cluster analysis, six clusters were classified. In the case of inflow from Shandong Province (C3), the contributions of secondary nitrate and secondary sulfate were higher than in other clusters. In addition, all days in this cluster during the heating season of North China corresponded to HCEs in Seoul. For inflow

through Northeast China and North Korea (C2, C5, and C6), the contribution of biomass burning source increased.

In the PSCF of $PM_{1.0}$ and $PM_{2.5-1.0}$ during SMP, North China Plain was shown to be a possible source area of secondary nitrate. For secondary sulfate during SMP, this area was shown only in $PM_{1.0}$. For Non-SMP, the influences from Shandong province and ship emissions were shown.

The contribution of secondary sources significantly increased when HCEs occurred. Since all days except one day correspond to the heating season of North China when the NO_X and SO_2 emissions of the region increase, long-range transport from the region was likely to influence the increase in contribution when HCEs occurred. In particular, secondary sulfate did not significantly increase in $PM_{2.5-1.0}$, but significantly increased in $PM_{1.0}$ when HCEs occurred. The possible source area of secondary sulfate for $PM_{1.0}$ during SMP was North China Plain, and the characteristics of sulfate source indicated the importance of foreign influences during winter. These results showed that $PM_{1.0}$ emitted from North China Plain was likely to contribute to the significant increase in contribution of secondary sulfate when HCEs occurred in Seoul during winter. In addition, it was shown that the ratio of $PM_{1.0}$ in secondary sulfate increased when HCEs occurred. Further research into the $PM_{1.0}/PM_{2.5}$ contribution ratio of secondary sulfate would contribute to evaluating the influence on Seoul from North China Plain. The contribution of biomass burning in $PM_{2.5-1.0}$ significantly increased when HCEs occurred. The PSCF of biomass burning in $PM_{2.5-1.0}$ indicated the North China Plain as a possible source area. This result implicated that $PM_{2.5-1.0}$ was an important portion in transported biomass burning sources. However, it is necessary to consider the coagulations of particles.

The DTTv of $PM_{2.5}$ and $PM_{1.0}$ during SMP were 0.611 nmol/min/m^3 and 0.588 nmol/min/m^3. About 96% of oxidative potential in $PM_{2.5}$ was the influence of $PM_{1.0}$. In the value normalized by mass concentration, $PM_{1.0}$ had a higher value than $PM_{2.5}$. For both $PM_{2.5}$ and $PM_{1.0}$, OC had the highest correlation with DTTv. NO_3^-, NH_4^+,

Mn, Fe, Zn, and Pb also had high correlation with DTTv. Secondary nitrate, biomass burning, industry, and coal combustion were selected as variables representing DTTv of $PM_{2.5}$. For $PM_{1.0}$, Secondary nitrate, biomass burning, incinerator, and soil were selected. Secondary nitrate and biomass burning were the common variables, and other variables were selected differently due to trace elements. Secondary nitrate represented the influence from secondary aerosol formation, and biomass burning was a representative source related to oxidative potential.

In conclusion, studying $PM_{1.0}$ as well as $PM_{2.5}$ helped understand the characteristics of $PM_{2.5}$ sources such as mobile and industry. In addition, the research into $PM_{1.0}$ contributed to evaluating influences of transported secondary sulfate when HCEs occurred during winter. $PM_{1.0}$ was known to be penetrated into lung deeper than $PM_{2.5}$ (Samek et al. 2018), and had higher oxidative potential per mass concentration in this study. Thus, the research into $PM_{1.0}$ is also needed in terms of health effects. Secondary sources contributed greatly to $PM_{2.5}$ and $PM_{1.0}$ in Seoul (especially $PM_{1.0}$), and the foreign influence on these sources was indicated. In addition, secondary aerosol formation process contributed to the oxidative potential of particulate matter. Thus, it is necessary to manage these sources. For this, it will be necessary to manage the gaseous precursors (NO_X, SO_2). However, according to recent studies, when NO_X emissions were reduced with COVID-19 lockdown, secondary particulate matter decreased less than expected and O_3 increased. Because of this, the studies suggested that not only NO_X but also NH_3 and VOCs should be considered to manage particulate matter and O_3 (Balamurugan et al. 2022; Huang et al. 2021; C. Zhang and Stevenson 2022).

Biomass burning is known as an important source of particulate matter in Seoul. In this study, biomass burning significantly increased in HCEs. Also, it was an important source related to oxidative potential like other studies. Thus, this source needs to be managed in Seoul. In future research, the OC speciation from organic compound analysis is necessary for more detailed interpretation of biomass burning source. In particular, from this OC speciation, it will be possible to verify the transport characteristics by distinguishing local and transported biomass burning (B.

M. Kim et al. 2016). In addition, comparing the results of this study with the research into $PM_{2.5}$ and $PM_{1.0}$ in possible source areas during the same period will contribute to understanding characteristics such as coagulation during transport (Sakamoto et al. 2016). In other future studies, it is necessary to verify the influence of Asian dust in spring and to compare the oxidative potential in different seasons.

References

Apeagyei, Eric, Michael S. Bank, and John D. Spengler. 2011. “Distribution of Heavy Metals in Road Dust along an Urban-Rural Gradient in Massachusetts.” *Atmospheric Environment* 45 (13): 2310–23. https://doi.org/10.1016/j.atmosenv.2010.11.015.

Araujo, Jesus A., and Andre E. Nel. 2009. “Particulate Matter and Atherosclerosis: Role of Particle Size, Composition and Oxidative Stress.” *Particle and Fibre Toxicology* 6: 1–19. https://doi.org/10.1186/1743-8977-6-24.

Balamurugan, Vigneshkumar, Jia Chen, Zhen Qu, Xiao Bi, and Frank N Keutsch. 2022. “Secondary PM Decreases Significantly Less than NO 2 Emission Reductions during COVID Lockdown in Germany,” no. 2: 1–33.

Bates, Josephine T., Ting Fang, Vishal Verma, Linghan Zeng, Rodney J. Weber, Paige E. Tolbert, Joseph Y. Abrams, et al. 2019. “Review of Acellular Assays of Ambient Particulate Matter Oxidative Potential: Methods and Relationships with Composition, Sources, and Health Effects.” *Environmental Science and Technology* 53 (8): 4003–19. https://doi.org/10.1021/acs.est.8b03430.

Bates, Josephine T., Rodney J. Weber, Joseph Abrams, Vishal Verma, Ting Fang, Mitchel Klein, Matthew J. Strickland, et al. 2015. “Reactive Oxygen Species Generation Linked to Sources of Atmospheric Particulate Matter and Cardiorespiratory Effects.” *Environmental Science and Technology* 49 (22): 13605–12. https://doi.org/10.1021/acs.est.5b02967.

Batmunkh, Tsatsral, Young J. Kim, Jin Sang Jung, Kihong Park, and Bulgan Tumendemberel. 2013. “Chemical Characteristics of Fine Particulate Matters Measured during Severe Winter Haze Events in Ulaanbaatar, Mongolia.” *Journal of the Air and Waste Management Association* 63 (6): 659–70. https://doi.org/10.1080/10962247.2013.776997.

Brown, Steven G., Shelly Eberly, Pentti Paatero, and Gary A. Norris. 2015. “Methods for Estimating Uncertainty in PMF Solutions: Examples with Ambient Air and Water Quality Data and Guidance on Reporting PMF Results.” *Science of the Total Environment* 518–519: 626–35. https://doi.org/10.1016/j.scitotenv.2015.01.022.

Chen, Chunrong, Haixu Zhang, Haiyan Li, Nana Wu, and Qiang Zhang. 2020. “Chemical Characteristics and Source Apportionment of Ambient PM1.0 and PM2.5 in a Polluted City in North China Plain.” *Atmospheric Environment* 242 (April): 117867. https://doi.org/10.1016/j.atmosenv.2020.117867.

Chen, Gongbo, Shanshan Li, Yongming Zhang, Wenyi Zhang, Daowei Li, Xuemei Wei, Yong He, et al. 2017. “Effects of Ambient PM1 Air Pollution on Daily Emergency Hospital Visits in China: An Epidemiological Study.” *The Lancet*

Planetary Health 1 (6): e221–29. https://doi.org/10.1016/S2542-5196(17)30100-6.

Chen, Gongbo, Lidia Morawska, Wenyi Zhang, Shanshan Li, Wei Cao, Hongyan Ren, Boguang Wang, et al. 2018. "Spatiotemporal Variation of PM1 Pollution in China." *Atmospheric Environment* 178 (January): 198–205. https://doi.org/10.1016/j.atmosenv.2018.01.053.

Choi, Jong kyu, Jong Bae Heo, Soo Jin Ban, Seung Muk Yi, and Kyung Duk Zoh. 2013. "Source Apportionment of PM2.5 at the Coastal Area in Korea." *Science of the Total Environment* 447: 370–80. https://doi.org/10.1016/j.scitotenv.2012.12.047.

Dai, Qili, Xiaohui Bi, Baoshuang Liu, Liwei Li, Jing Ding, Wenbin Song, Shiyang Bi, et al. 2018. "Chemical Nature of PM2.5 and PM10 in Xi'an, China: Insights into Primary Emissions and Secondary Particle Formation." *Environmental Pollution* 240: 155–66. https://doi.org/10.1016/j.envpol.2018.04.111.

Duan, Fengkui, Xiande Liu, Tong Yu, and Hélène Cachier. 2004. "Identification and Estimate of Biomass Burning Contribution to the Urban Aerosol Organic Carbon Concentrations in Beijing." *Atmospheric Environment* 38 (9): 1275–82. https://doi.org/10.1016/j.atmosenv.2003.11.037.

Duan, Jingchun, Jihua Tan, Shulan Wang, Jimin Hao, and Fahe Chai. 2012. "Size Distributions and Sources of Elements in Particulate Matter at Curbside, Urban and Rural Sites in Beijing." *Journal of Environmental Sciences* 24 (1): 87–94. https://doi.org/10.1016/S1001-0742(11)60731-6.

Fang, T., V. Verma, H. Guo, L. E. King, E. S. Edgerton, and R. J. Weber. 2015. "A Semi-Automated System for Quantifying the Oxidative Potential of Ambient Particles in Aqueous Extracts Using the Dithiothreitol (DTT) Assay: Results from the Southeastern Center for Air Pollution and Epidemiology (SCAPE)." *Atmospheric Measurement Techniques* 8 (1): 471–82. https://doi.org/10.5194/amt-8-471-2015.

Farina, Francesca, Giulio Sancini, Eleonora Longhin, Paride Mantecca, Marina Camatini, and Paola Palestini. 2013. "Milan PM1 Induces Adverse Effects on Mice Lungs and Cardiovascular System." *BioMed Research International* 2013. https://doi.org/10.1155/2013/583513.

Feng, Xiaolei, Longyi Shao, Tim Jones, Yaowei Li, Yaxin Cao, Mengyuan Zhang, Shuoyi Ge, Cheng Xue Yang, Jing Lu, and Kelly BéruBé. 2022. "Oxidative Potential and Water-Soluble Heavy Metals of Size-Segregated Airborne Particles in Haze and Non-Haze Episodes: Impact of the 'Comprehensive Action Plan' in China." *Science of the Total Environment* 814. https://doi.org/10.1016/j.scitotenv.2021.152774.

Fourtziou, L., E. Liakakou, I. Stavroulas, C. Theodosi, P. Zarmpas, B. Psiloglou, J.

Sciare, et al. 2017. “Multi-Tracer Approach to Characterize Domestic Wood Burning in Athens (Greece) during Wintertime.” *Atmospheric Environment* 148: 89–101. https://doi.org/10.1016/j.atmosenv.2016.10.011.

Franck, Ulrich, Siad Odeh, Alfred Wiedensohler, Birgit Wehner, and Olf Herbarth. 2011. “The Effect of Particle Size on Cardiovascular Disorders - The Smaller the Worse.” *Science of the Total Environment* 409 (20): 4217–21. https://doi.org/10.1016/j.scitotenv.2011.05.049.

Heo, J. B., P. K. Hopke, and S. M. Yi. 2009. “Source Apportionment of PM2.5 in Seoul, Korea.” *Atmospheric Chemistry and Physics* 9 (14): 4957–71. https://doi.org/10.5194/acp-9-4957-2009.

Heo, Jongbae, James J. Schauer, Okhee Yi, Domyung Paek, Ho Kim, and Seung Muk Yi. 2014. “Fine Particle Air Pollution and Mortality: Importance of Specific Sources and Chemical Species.” *Epidemiology* 25 (3): 379–88. https://doi.org/10.1097/EDE.0000000000000044.

Hien, Pham Duy, Vuong Thu Bac, Nguyen Thi Hong Thinh, Ha Lan Anh, Duong Duc Thang, and Nguyen The Nghia. 2021. “A Comparison Study of Chemical Compositions and Sources of Pm1.0 and Pm2.5 in Hanoi.” *Aerosol and Air Quality Research* 21 (10). https://doi.org/10.4209/AAQR.210056.

Hu, Jianlin, Yungang Wang, Qi Ying, and Hongliang Zhang. 2014. “Spatial and Temporal Variability of PM2.5 and PM10 over the North China Plain and the Yangtze River Delta, China.” *Atmospheric Environment* 95: 598–609. https://doi.org/10.1016/j.atmosenv.2014.07.019.

Huang, Xin, Aijun Ding, Jian Gao, Bo Zheng, Derong Zhou, Ximeng Qi, Rong Tang, et al. 2021. “Enhanced Secondary Pollution Offset Reduction of Primary Emissions during COVID-19 Lockdown in China.” *National Science Review* 8 (2). https://doi.org/10.1093/nsr/nwaa137.

Hueglin, Christoph, Robert Gehrig, Urs Baltensperger, Martin Gysel, Christian Monn, and Heinz Vonmont. 2005. “Chemical Characterisation of PM2.5, PM10 and Coarse Particles at Urban, near-City and Rural Sites in Switzerland.” *Atmospheric Environment* 39 (4): 637–51. https://doi.org/10.1016/j.atmosenv.2004.10.027.

Iijima, Akihiro, Keiichi Sato, Kiyoko Yano, Hiroshi Tago, Masahiko Kato, Hirokazu Kimura, and Naoki Furuta. 2007. “Particle Size and Composition Distribution Analysis of Automotive Brake Abrasion Dusts for the Evaluation of Antimony Sources of Airborne Particulate Matter.” *Atmospheric Environment* 41 (23): 4908–19. https://doi.org/10.1016/j.atmosenv.2007.02.005.

Jiang, Huanhuan, C. M. Sabbir Ahmed, Alexa Canchola, Jin Y. Chen, and Ying Hsuan Lin. 2019. “Use of Dithiothreitol Assay to Evaluate the Oxidative Potential of Atmospheric Aerosols.” *Atmosphere* 10 (10): 1–21.

https://doi.org/10.3390/atmos10100571.

Jung, Jinsang, Sangil Lee, Hyosun Kim, Doyeon Kim, Hyoeun Lee, and Sanghyup Oh. 2014. “Quantitative Determination of the Biomass-Burning Contribution to Atmospheric Carbonaceous Aerosols in Daejeon, Korea, during the Rice-Harvest Period.” *Atmospheric Environment* 89: 642–50. https://doi.org/10.1016/j.atmosenv.2014.03.010.

Kang, Byung-Wook, Min-Ji Kim, Kyung-Min Baek, Young-Kyo Seo, Hak Sung Lee, Jong-Ho Kim, and Jin-Seok Han. 2018. “A Study on the Concentration Distribution of Airborne Heavy Metals in Major Industrial Complexes in Korea.” *Journal of Korean Society for Atmospheric Environment* 34 (2): 269–80. https://doi.org/10.5572/kosae.2018.34.2.269.

Khan, Jahan Zeb, Long Sun, Yingze Tian, Guoliang Shi, and Yinchang Feng. 2021. “Chemical Characterization and Source Apportionment of PM1 and PM2.5 in Tianjin, China: Impacts of Biomass Burning and Primary Biogenic Sources.” *Journal of Environmental Sciences (China)* 99: 196–209. https://doi.org/10.1016/j.jes.2020.06.027.

Kim, Bong Mann, Jihoon Seo, Jin Young Kim, Ji Yi Lee, and Yumi Kim. 2016. “Transported vs. Local Contributions from Secondary and Biomass Burning Sources to PM2.5.” *Atmospheric Environment* 144: 24–36. https://doi.org/10.1016/j.atmosenv.2016.08.072.

Kim, Hwajin, Qi Zhang, Bae Gwi-Nam, Jin Young Kim, and Seung Bok Lee. 2017. “Sources and Atmospheric Processing of Winter Aerosols in Seoul, Korea: Insights from Real-Time Measurements Using a High-Resolution Aerosol Mass Spectrometer.” *Atmospheric Chemistry and Physics* 17 (3): 2009–33. https://doi.org/10.5194/acp-17-2009-2017.

Kim, Hwajin, Qi Zhang, and Jongbae Heo. 2018. “Influence of Intense Secondary Aerosol Formation and Long-Range Transport on Aerosol Chemistry and Properties in the Seoul Metropolitan Area during Spring Time: Results from KORUS-AQ.” *Atmospheric Chemistry and Physics* 18 (10): 7149–68. https://doi.org/10.5194/acp-18-7149-2018.

Kim, In Sun, Ji Yi Lee, and Yong Pyo Kim. 2013. “Impact of Polycyclic Aromatic Hydrocarbon (PAH) Emissions from North Korea to the Air Quality in the Seoul Metropolitan Area, South Korea.” *Atmospheric Environment* 70 (2013): 159–65. https://doi.org/10.1016/j.atmosenv.2012.12.040.

Kim, Sunhye, Tae Young Kim, Seung Muk Yi, and Jongbae Heo. 2018. “Source Apportionment of PM2.5 Using Positive Matrix Factorization (PMF) at a Rural Site in Korea.” *Journal of Environmental Management* 214: 325–34. https://doi.org/10.1016/j.jenvman.2018.03.027.

Kim, Yumi, Jihoon Seo, Jin Young Kim, Ji Yi Lee, Hwajin Kim, and Bong Mann Kim. 2018. “Characterization of PM2.5 and Identification of Transported

Secondary and Biomass Burning Contribution in Seoul, Korea." *Environmental Science and Pollution Research* 25 (5): 4330–43. https://doi.org/10.1007/s11356-017-0772-x.

Kramer, Amanda J., Weruka Rattanavaraha, Zhenfa Zhang, Avram Gold, Jason D. Surratt, and Ying Hsuan Lin. 2016. "Assessing the Oxidative Potential of Isoprene-Derived Epoxides and Secondary Organic Aerosol." *Atmospheric Environment* 130: 211–18. https://doi.org/10.1016/j.atmosenv.2015.10.018.

Lee, Bok Jin, Se Chang Son, Geun Hye Yu, Seoryeong Ju, Seungshik Park, and Sangil Lee. 2020. "A Study on Oxidative Potential of Fine Particles Measured at an Urban Site and a Rural Site." *Journal of Korean Society for Atmospheric Environment* 36 (6): 727–41. https://doi.org/10.5572/KOSAE.2020.36.6.727.

Lee, Jong Hoon, and Philip K. Hopke. 2006. "Apportioning Sources of PM2.5 in St. Louis, MO Using Speciation Trends Network Data." *Atmospheric Environment* 40 (SUPPL. 2): 360–77. https://doi.org/10.1016/j.atmosenv.2005.11.074.

Lee, S. C., Y. Cheng, K. F. Ho, J. J. Cao, P. K.K. Louie, J. C. Chow, and J. G. Watson. 2006. "PM1.0 and PM2.5 Characteristics in the Roadside Environment of Hong Kong." *Aerosol Science and Technology* 40 (3): 157–65. https://doi.org/10.1080/02786820500494544.

Liang, Xiaoxue, Tao Huang, Siying Lin, Jinxiang Wang, Jingyue Mo, Hong Gao, Zhanxiang Wang, Jixiang Li, Lulu Lian, and Jianmin Ma. 2019. "Chemical Composition and Source Apportionment of PM 1 and PM 2.5 in a National Coal Chemical Industrial Base of the Golden Energy Triangle, Northwest China." *Science of the Total Environment* 659: 188–99. https://doi.org/10.1016/j.scitotenv.2018.12.335.

Lin, Yuan Chung, Ya Ching Li, Kassian T.T. Amesho, Sumarlin Shangdiar, Feng Chih Chou, and Pei Cheng Cheng. 2020. "Chemical Characterization of PM2.5 Emissions and Atmospheric Metallic Element Concentrations in PM2.5 Emitted from Mobile Source Gasoline-Fueled Vehicles." *Science of the Total Environment* 739: 139942. https://doi.org/10.1016/j.scitotenv.2020.139942.

Long, Shilei, Jianrong Zeng, Yan Li, Liangman Bao, Lingling Cao, Ke Liu, Liang Xu, et al. 2014. "Characteristics of Secondary Inorganic Aerosol and Sulfate Species in Size-Fractionated Aerosol Particles in Shanghai." *Journal of Environmental Sciences (China)* 26 (5): 1040–51. https://doi.org/10.1016/S1001-0742(13)60521-5.

Luo, Li, Yong-Yun Zhang, Hua-Yun Xiao, Hong-Wei Xiao, Neng-Jian Zheng, Zhong-Yi Zhang, Ya-Jun Xie, and Cheng Liu. 2019. "Spatial Distributions and Sources of Inorganic Chlorine in PM2.5 across China in Winter" Atmosphere 10, no. 9: 505. https://doi.org/10.3390/atmos10090505

Ma, Yiqiu, Yubo Cheng, Xinghua Qiu, Gang Cao, Yanhua Fang, Junxia Wang, Tong Zhu, Jianzhen Yu, and Di Hu. 2018. “Sources and Oxidative Potential of Water-Soluble Humic-like Substances (HULISWS) in Fine Particulate Matter (PM2.5) in Beijing.” *Atmospheric Chemistry and Physics* 18 (8): 5607–17. https://doi.org/10.5194/acp-18-5607-2018.

Mabato, Beatrix Rosette Go, Yan Lyu, Yan Ji, Yong Jie Li, Dan Dan Huang, Xue Li, Theodora Nah, Chun Ho Lam, and Chak K. Chan. 2022. “Aqueous Secondary Organic Aerosol Formation from the Direct Photosensitized Oxidation of Vanillin in the Absence and Presence of Ammonium Nitrate.” *Atmospheric Chemistry and Physics* 22 (1): 273–93. https://doi.org/10.5194/acp-22-273-2022.

MacIejczyk, Polina, Mianhua Zhong, Morton Lippmann, and Lung Chi Chen. 2010. “Oxidant Generation Capacity of Source-Apportioned PM2.5.” *Inhalation Toxicology* 22 (SUPPL. 2): 29–36. https://doi.org/10.3109/08958378.2010.509368.

Meng, Kai, Xiangde Xu, Xinghong Cheng, Xiaobin Xu, Xiaoli Qu, Wenhui Zhu, Cuiping Ma, Yuling Yang, and Yuguang Zhao. 2018. “Spatio-Temporal Variations in SO2 and NO2 Emissions Caused by Heating over the Beijing-Tianjin-Hebei Region Constrained by an Adaptive Nudging Method with OMI Data.” *Science of the Total Environment* 642 (2): 543–52. https://doi.org/10.1016/j.scitotenv.2018.06.021.

Miller-Schulze, Justin P., Martin Shafer, James J. Schauer, Jongbae Heo, Paul A. Solomon, Jeffrey Lantz, Maria Artamonova, et al. 2015. “Seasonal Contribution of Mineral Dust and Other Major Components to Particulate Matter at Two Remote Sites in Central Asia.” *Atmospheric Environment* 119: 11–20. https://doi.org/10.1016/j.atmosenv.2015.07.011.

Nunes, R. A.O., M. C.M. Alvim-Ferraz, F. G. Martins, and S. I.V. Sousa. 2017. “The Activity-Based Methodology to Assess Ship Emissions - A Review.” *Environmental Pollution* 231 (x): 87–103. https://doi.org/10.1016/j.envpol.2017.07.099.

Pan, Yun, Zhiming Wu, Jizhi Zhou, Jun Zhao, Xiuxiu Ruan, Jianyong Liu, and Guangren Qian. 2013. “Chemical Characteristics and Risk Assessment of Typical Municipal Solid Waste Incineration (MSWI) Fly Ash in China.” *Journal of Hazardous Materials* 261: 269–76. https://doi.org/10.1016/j.jhazmat.2013.07.038.

Pang, Nini, Jian Gao, Fei Che, Tong Ma, Su Liu, Yan Yang, Pusheng Zhao, et al. 2020. “Cause of PM2.5 Pollution during the 2016-2017 Heating Season in Beijing, Tianjin, and Langfang, China.” *Journal of Environmental Sciences (China)* 95 (x): 201–9. https://doi.org/10.1016/j.jes.2020.03.024.

Park, Eun Ha, Jongbae Heo, Ho Kim, and Seung Muk Yi. 2020. “Long Term Trends of Chemical Constituents and Source Contributions of PM2.5 in

Seoul." *Chemosphere* 251: 126371. https://doi.org/10.1016/j.chemosphere.2020.126371.

Park, Jieun, Hyewon Kim, Youngkwon Kim, Jongbae Heo, Sang-Woo Kim, Kwonho Jeon, Seung-Muk Yi, and Philip K. Hopke. 2022. "Source Apportionment of PM2.5 in Seoul, South Korea and Beijing, China Using Dispersion Normalized PMF." *Science of The Total Environment* 833 (April): 155056. https://doi.org/10.1016/j.scitotenv.2022.155056.

Park, Jieun, Eun Ha Park, James J. Schauer, Seung Muk Yi, and Jongbae Heo. 2018. "Reactive Oxygen Species (ROS) Activity of Ambient Fine Particles (PM2.5) Measured in Seoul, Korea." *Environment International* 117 (December 2017): 276–83. https://doi.org/10.1016/j.envint.2018.05.018.

Park, Jong-Moon, Tae-Jung Lee, and Dong-Sool Kim. 2022. "Improving PMF Source Reconciliation with Cluster Analysis for PM2.5 Hourly Data from Seoul, Korea." *Atmospheric Pollution Research* 13 (5): 101398. https://doi.org/10.1016/j.apr.2022.101398.

Park, Min Bin, Tae Jung Lee, Eun Sun Lee, and Dong Sool Kim. 2019. "Enhancing Source Identification of Hourly PM2.5 Data in Seoul Based on a Dataset Segmentation Scheme by Positive Matrix Factorization (PMF)." *Atmospheric Pollution Research* 10 (4): 1042–59. https://doi.org/10.1016/j.apr.2019.01.013.

Pey, Jorge, Noemí Pérez, Joaquim Cortés, Andrés Alastuey, and Xavier Querol. 2013. "Chemical Fingerprint and Impact of Shipping Emissions over a Western Mediterranean Metropolis: Primary and Aged Contributions." *Science of the Total Environment* 463–464: 497–507. https://doi.org/10.1016/j.scitotenv.2013.06.061.

Qiao, Ting, Mengfei Zhao, Guangli Xiu, and Jianzhen Yu. 2015. "Seasonal Variations of Water Soluble Composition (WSOC, Hulis and WSIIs) in PM1 and Its Implications on Haze Pollution in Urban Shanghai, China." *Atmospheric Environment* 123: 306–14. https://doi.org/10.1016/j.atmosenv.2015.03.010.

Ray, Paul D., Bo Wen Huang, and Yoshiaki Tsuji. 2012. "Reactive Oxygen Species (ROS) Homeostasis and Redox Regulation in Cellular Signaling." *Cellular Signalling* 24 (5): 981–90. https://doi.org/10.1016/j.cellsig.2012.01.008.

Ryu, Nahyeon, Hyungseok Kim, and Pilsung Kang. 2016. "Evaluating Variable Selection Techniques for Multivariate Linear Regression." *Journal of Korean Institute of Industrial Engineers* 42 (5): 314–26. https://doi.org/10.7232/jkiie.2016.42.5.314.

Saffari, Arian, Nancy Daher, Martin M. Shafer, James J. Schauer, and Constantinos Sioutas. 2014. "Seasonal and Spatial Variation in Dithiothreitol (DTT)

Activity of Quasi-Ultrafine Particles in the Los Angeles Basin and Its Association with Chemical Species." *Journal of Environmental Science and Health - Part A Toxic/Hazardous Substances and Environmental Engineering* 49 (4): 441–51. https://doi.org/10.1080/10934529.2014.854677.

Sakamoto, Kimiko M., James R. Laing, Robin G. Stevens, Daniel A. Jaffe, and Jeffrey R. Pierce. 2016. "The Evolution of Biomass-Burning Aerosol Size Distributions Due to Coagulation: Dependence on Fire and Meteorological Details and Parameterization." *Atmospheric Chemistry and Physics* 16 (12): 7709–24. https://doi.org/10.5194/acp-16-7709-2016.

Samek, Lucyna, Zdzislaw Stegowski, Katarzyna Styszko, Leszek Furman, and Joanna Fiedor. 2018. "Seasonal Contribution of Assessed Sources to Submicron and Fine Particulate Matter in a Central European Urban Area." *Environmental Pollution* 241: 406–11. https://doi.org/10.1016/j.envpol.2018.05.082.

Strak, Maciej, Nicole Janssen, Rob Beelen, Oliver Schmitz, Ilonca Vaartjes, Derek Karssenberg, Carolien van den Brink, et al. 2017. "Long-Term Exposure to Particulate Matter, NO2 and the Oxidative Potential of Particulates and Diabetes Prevalence in a Large National Health Survey." *Environment International* 108 (2): 228–36. https://doi.org/10.1016/j.envint.2017.08.017.

Sylvestre, Alexandre, Aurélie Mizzi, Sébastien Mathiot, Fanny Masson, Jean L. Jaffrezo, Julien Dron, Boualem Mesbah, Henri Wortham, and Nicolas Marchand. 2017. "Comprehensive Chemical Characterization of Industrial PM2.5from Steel Industry Activities." *Atmospheric Environment* 152: 180–90. https://doi.org/10.1016/j.atmosenv.2016.12.032.

Taiwo, Adewale M., David C.S. Beddows, Zongbo Shi, and Roy M. Harrison. 2014. "Mass and Number Size Distributions of Particulate Matter Components: Comparison of an Industrial Site and an Urban Background Site." *Science of the Total Environment* 475: 29–38. https://doi.org/10.1016/j.scitotenv.2013.12.076.

Thorpe, Alistair, and Roy M. Harrison. 2008. "Sources and Properties of Non-Exhaust Particulate Matter from Road Traffic: A Review." *Science of the Total Environment* 400 (1–3): 270–82. https://doi.org/10.1016/j.scitotenv.2008.06.007.

Uria-Tellaetxe, Iratxe, and David C. Carslaw. 2014. "Conditional Bivariate Probability Function for Source Identification." *Environmental Modelling and Software* 59: 1–9. https://doi.org/10.1016/j.envsoft.2014.05.002.

Verma, Vishal, Ting Fang, Lu Xu, Richard E. Peltier, Armistead G. Russell, Nga Lee Ng, and Rodney J. Weber. 2015. "Organic Aerosols Associated with the Generation of Reactive Oxygen Species (ROS) by Water-Soluble PM2.5." *Environmental Science and Technology* 49 (7): 4646–56. https://doi.org/10.1021/es505577w.

Viana, M., T. A.J. Kuhlbusch, X. Querol, A. Alastuey, R. M. Harrison, P. K. Hopke, W. Winiwarter, et al. 2008. “Source Apportionment of Particulate Matter in Europe: A Review of Methods and Results.” *Journal of Aerosol Science* 39 (10): 827–49. https://doi.org/10.1016/j.jaerosci.2008.05.007.

Vreeland, Heidi, Rodney Weber, Michael Bergin, Roby Greenwald, Rachel Golan, Armistead G. Russell, Vishal Verma, and Jeremy A. Sarnat. 2017. “Oxidative Potential of PM2.5 during Atlanta Rush Hour: Measurements of in-Vehicle Dithiothreitol (DTT) Activity.” *Atmospheric Environment* 165: 169–78. https://doi.org/10.1016/j.atmosenv.2017.06.044.

Waked, A., O. Favez, L. Y. Alleman, C. Piot, J. E. Petit, T. Delaunay, E. Verlinden, et al. 2014. “Source Apportionment of PM10 in a North-Western Europe Regional Urban Background Site (Lens, France) Using Positive Matrix Factorization and Including Primary Biogenic Emissions.” *Atmospheric Chemistry and Physics* 14 (7): 3325–46. https://doi.org/10.5194/acp-14-3325-2014.

Wang, Dongfang, Bin Zhou, Qingyan Fu, Qianbiao Zhao, Qi Zhang, Jianmin Chen, Xin Yang, Yusen Duan, and Juan Li. 2016. “Intense Secondary Aerosol Formation Due to Strong Atmospheric Photochemical Reactions in Summer: Observations at a Rural Site in Eastern Yangtze River Delta of China.” *Science of the Total Environment* 571: 1454–66. https://doi.org/10.1016/j.scitotenv.2016.06.212.

Wang, Guangzhi, Yuanyuan Xu, Likun Huang, Kun Wang, Hairui Shen, and Zhe Li. 2021. “Pollution Characteristics and Toxic Effects of PM1.0 and PM2.5 in Harbin, China.” *Environmental Science and Pollution Research* 28 (11): 13229–42. https://doi.org/10.1007/s11356-020-11510-8.

Wang, Jingpeng, Xin Lin, Liping Lu, Yujie Wu, Huanxin Zhang, Qi Lv, Weiping Liu, Yanlin Zhang, and Shulin Zhuang. 2019. “Temporal Variation of Oxidative Potential of Water Soluble Components of Ambient PM2.5 Measured by Dithiothreitol (DTT) Assay.” *Science of the Total Environment* 649: 969–78. https://doi.org/10.1016/j.scitotenv.2018.08.375.

Wang, Junfeng, Ye Qiu, Shutong He, Nan Liu, Chengyu Xiao, and Lingxuan Liu. 2018. “Investigating the Driving Forces of NOx Generation from Energy Consumption in China.” *Journal of Cleaner Production* 184: 836–46. https://doi.org/10.1016/j.jclepro.2018.02.305.

Wang, Li, Fengying Zhang, Eva Pilot, Jie Yu, Chengjing Nie, Jennifer Holdaway, Linsheng Yang, et al. 2018. “Taking Action on Air Pollution Control in the Beijing-Tianjin-Hebei (BTH) Region: Progress, Challenges and Opportunities.” *International Journal of Environmental Research and Public Health* 15 (2). https://doi.org/10.3390/ijerph15020306.

Warburton, David, Nicole Warburton, Clarence Wigfall, Ochir Chimedsuren, Delgerzul Lodoisamba, Sereeter Lodoysamba, and Badarch Jargalsaikhan.

2018. “Impact of Seasonal Winter Air Pollution on Health across the Lifespan in Mongolia and Some Putative Solutions.” *Annals of the American Thoracic Society* 15 (April): S86–90. https://doi.org/10.1513/AnnalsATS.201710-758MG.

Wen, Liang, Jianmin Chen, Lingxiao Yang, Xinfeng Wang, Caihong Xu, Xiao Sui, Lan Yao, et al. 2015. “Enhanced Formation of Fine Particulate Nitrate at a Rural Site on the North China Plain in Summer: The Important Roles of Ammonia and Ozone.” *Atmospheric Environment* 101: 294–302. https://doi.org/10.1016/j.atmosenv.2014.11.037.

Yang, Fumo, Boming Ye, Kebin He, Yongliang Ma, Steven H. Cadle, Tai Chan, and Patricia A. Mulawa. 2005. “Characterization of Atmospheric Mineral Components of PM2.5 in Beijing and Shanghai, China.” *Science of the Total Environment* 343 (1–3): 221–30. https://doi.org/10.1016/j.scitotenv.2004.10.017.

Yang, Hsi Hsien, Shao Wei Luo, Kuei Ting Lee, Jhin Yan Wu, Chun Wei Chang, and Pei Feng Chu. 2016. “Fine Particulate Speciation Profile and Emission Factor of Municipal Solid Waste Incinerator Established by Dilution Sampling Method.” *Journal of the Air and Waste Management Association* 66 (8): 807–14. https://doi.org/10.1080/10962247.2016.1184195.

Yu, Haoran, Jinlai Wei, Yilan Cheng, Kiran Subedi, and Vishal Verma. 2018. “Synergistic and Antagonistic Interactions among the Particulate Matter Components in Generating Reactive Oxygen Species Based on the Dithiothreitol Assay.” *Environmental Science and Technology* 52 (4): 2261–70. https://doi.org/10.1021/acs.est.7b04261.

Yu, Shuang Yu, Wei Jian Liu, Yun Song Xu, Kan Yi, Ming Zhou, Shu Tao, and Wen Xin Liu. 2019. “Characteristics and Oxidative Potential of Atmospheric PM2.5 in Beijing: Source Apportionment and Seasonal Variation.” *Science of the Total Environment* 650: 277–87. https://doi.org/10.1016/j.scitotenv.2018.09.021.

Zhang, Chenyue, and David Stevenson. 2022. “Characteristic Changes of Ozone and Its Precursors in London during COVID-19 Lockdown and the Ozone Surge Reason Analysis.” *Atmospheric Environment* 273 (January): 118980. https://doi.org/10.1016/j.atmosenv.2022.118980.

Zhang, Yanyan, Daniel Obrist, Barbara Zielinska, and Alan Gertler. 2013. “Particulate Emissions from Different Types of Biomass Burning.” *Atmospheric Environment* 72: 27–35. https://doi.org/10.1016/j.atmosenv.2013.02.026.

Zhang, Yanyun, Jianlei Lang, Shuiyuan Cheng, Shengyue Li, Ying Zhou, Dongsheng Chen, Hanyu Zhang, and Haiyan Wang. 2018. “Chemical Composition and Sources of PM1 and PM2.5 in Beijing in Autumn.” *Science of the Total Environment* 630: 72–82.

https://doi.org/10.1016/j.scitotenv.2018.02.151.

Zhao, H. Y., Q. Zhang, D. B. Guan, S. J. Davis, Z. Liu, H. Huo, J. T. Lin, W. D. Liu, and K. B. He. 2015. “Assessment of China’s Virtual Air Pollution Transport Embodied in Trade by Using a Consumption-Based Emission Inventory.” *Atmospheric Chemistry and Physics* 15 (10): 5443–56. https://doi.org/10.5194/acp-15-5443-2015.

Zhu, Chuanyong, Hezhong Tian, Ke Cheng, Kaiyun Liu, Kun Wang, Shenbing Hua, Jiajia Gao, and Junrui Zhou. 2016. “Potentials of Whole Process Control of Heavy Metals Emissions from Coal-Fired Power Plants in China.” *Journal of Cleaner Production* 114: 343–51. https://doi.org/10.1016/j.jclepro.2015.05.008.

Zong, Zheng, Xiaoping Wang, Chongguo Tian, Yingjun Chen, Shanfei Fu, Lin Qu, Ling Ji, Jun Li, and Gan Zhang. 2018. “PMF and PSCF Based Source Apportionment of PM2.5 at a Regional Background Site in North China.” *Atmospheric Research* 203 (November 2017): 207–15. https://doi.org/10.1016/j.atmosres.2017.12.013.

Supplementary

Table S1 Uncertainty calculation

	Uncertainty calculation
Mass concentration	$4 \times conc$
Carbonaceous species	$\sqrt{\left((0.05 + E) \times conc. + IDLs\right)^2 + (S.D.\ of\ Blank)^2}$
Ionic species	$\sqrt{(global\ unc. \times conc.)^2 + (S.D.\ of\ Blank)^2 + (E \times conc.)^2}$
Trace elements	$\sqrt{((0.1 + E) \times conc.)^2 + (0.5 \times MDL)^2}$
E : sampling error compared with 16.7 LPM	

Table S2 Results of multiple linear regression of $PM_{2.5}$

Model Summary

Model	R	R Square	Adjusted R Square	Std. Error of the Estimate	Durbin-Watson
7	.886	.786	.764	.044957738277494	2.124

ANOVA

Model		Sum of Squares	df	Mean Square	F	Sig.
7	Regression	.296	4	.074	36.665	.000[h]
	Residual	.081	40	.002		
	Total	.377	44			

Coefficients

Model		Unstandardized Coefficients		Standardized Coefficients	t	Sig.	Collinearity Statistics	
		B	Std. Error	Beta			Tolerance	VIF
7	(Constant)	.420	.028		15.038	.000		
	Industry	.022	.008	.218	2.610	.013	.765	1.307
	Biomass burning	.015	.005	.242	2.710	.010	.673	1.486
	Secondary nitrate	.007	.001	.575	7.300	.000	.865	1.157
	Coal combustion	.013	.003	.345	4.032	.000	.733	1.364

Table S3 Results of multiple linear regression of $PM_{1.0}$

Model Summary

Model	R	R Square	Adjusted R Square	Std. Error of the Estimate	Durbin-Watson
7	.745	.556	.511	.056533348854945	2.122

ANOVA

Model		Sum of Squares	df	Mean Square	F	Sig.
7	Regression	.160	4	.040	12.498	.000[h]
	Residual	.128	40	.003		
	Total	.288	44			

Coefficients

Model		Unstandardized Coefficients		Standardized Coefficients			Collinearity Statistics	
		B	Std. Error	Beta	t	Sig.	Tolerance	VIF
7	(Constant)	.416	.033		12.724	.000		
	Soil	.113	.037	.341	3.081	.004	.905	1.105
	Incinerator	.029	.014	.256	2.061	.046	.721	1.388
	Biomass burning	.013	.006	.243	2.044	.048	.789	1.268
	Secondary nitrate	.008	.002	.613	5.117	.000	.774	1.292

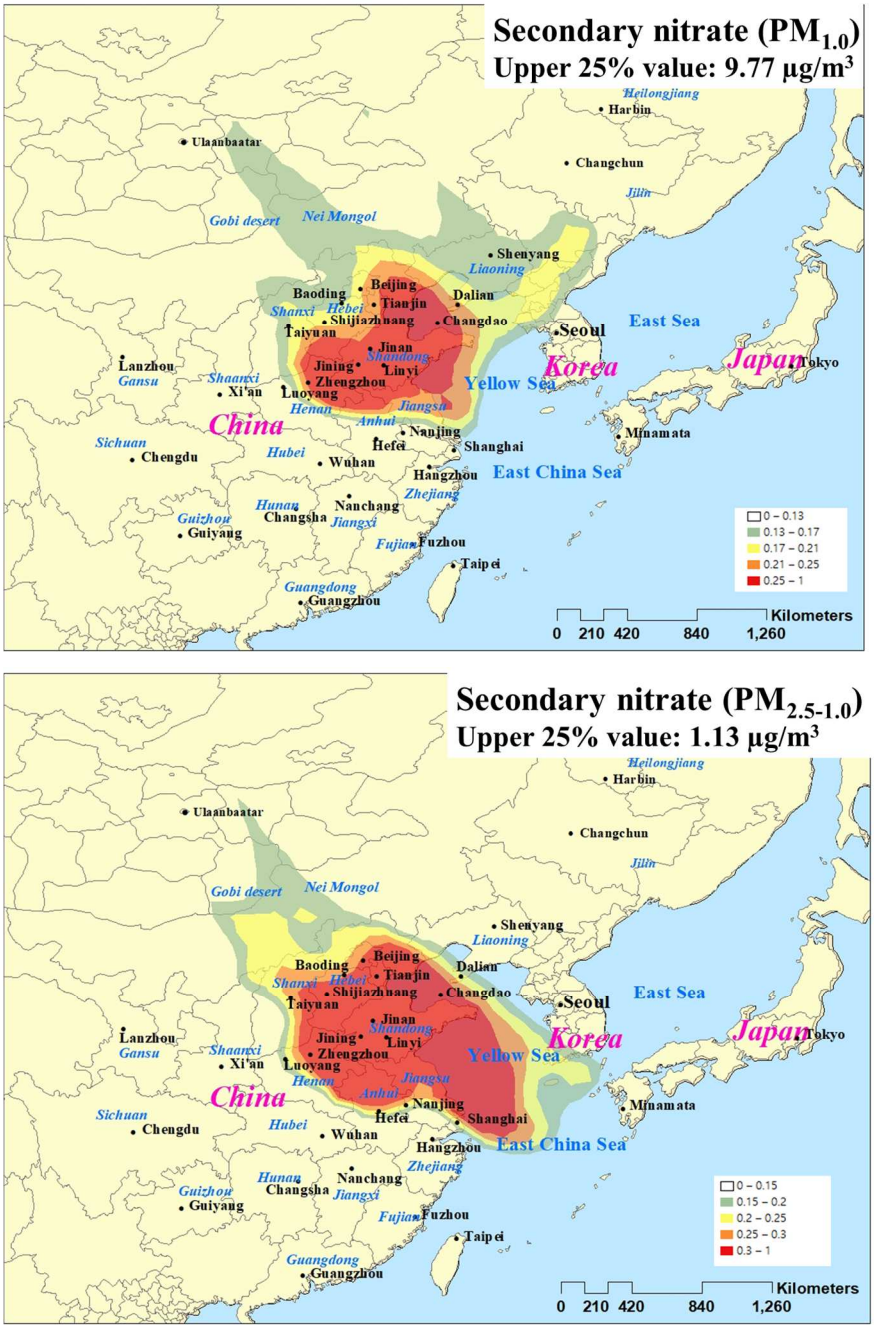

Figure S1 PSCF maps of secondary nitrate during sampling period

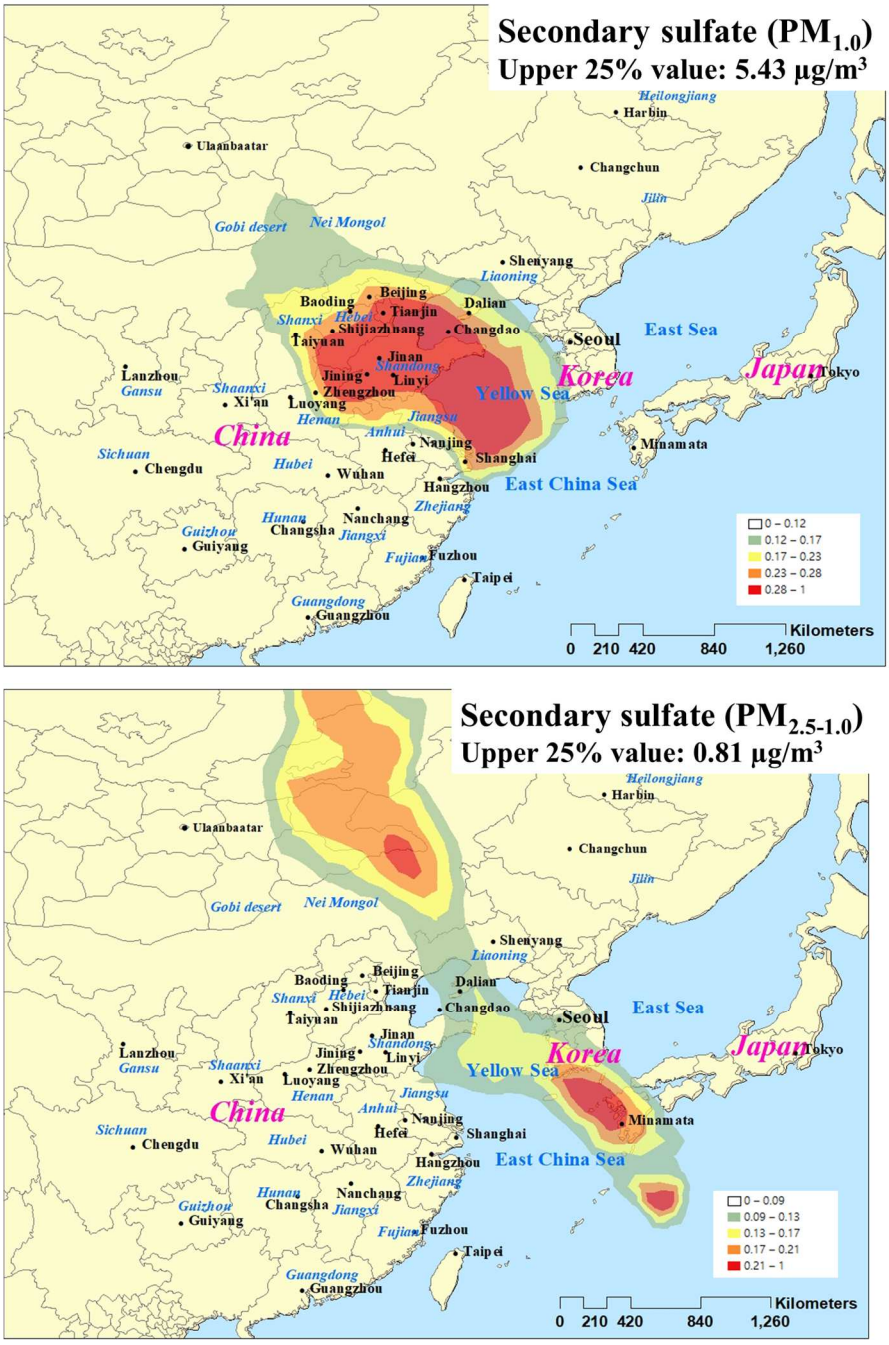

Figure S2 PSCF maps of secondary sulfate during sampling period

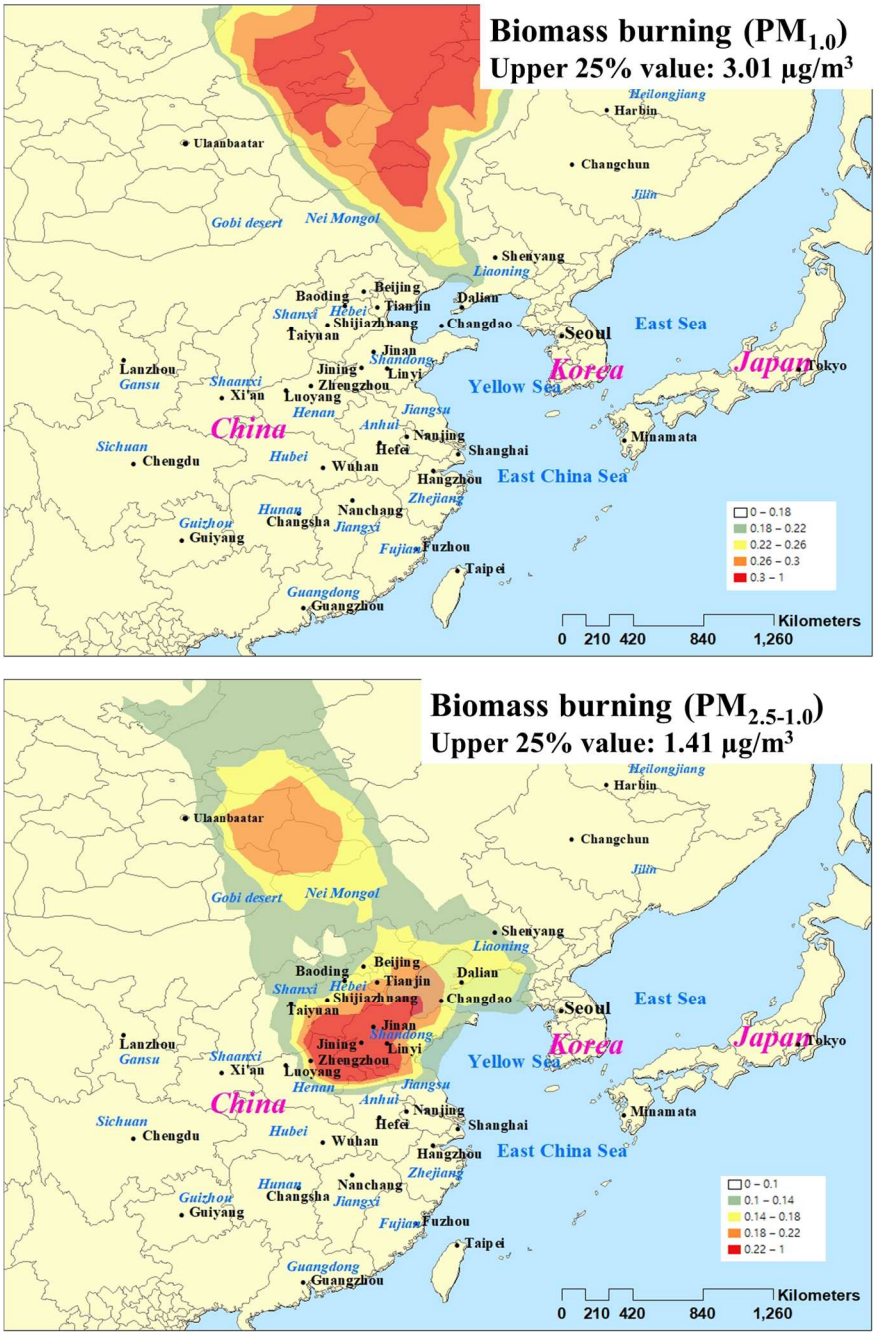

Figure S3 PSCF maps of biomass burning during sampling period

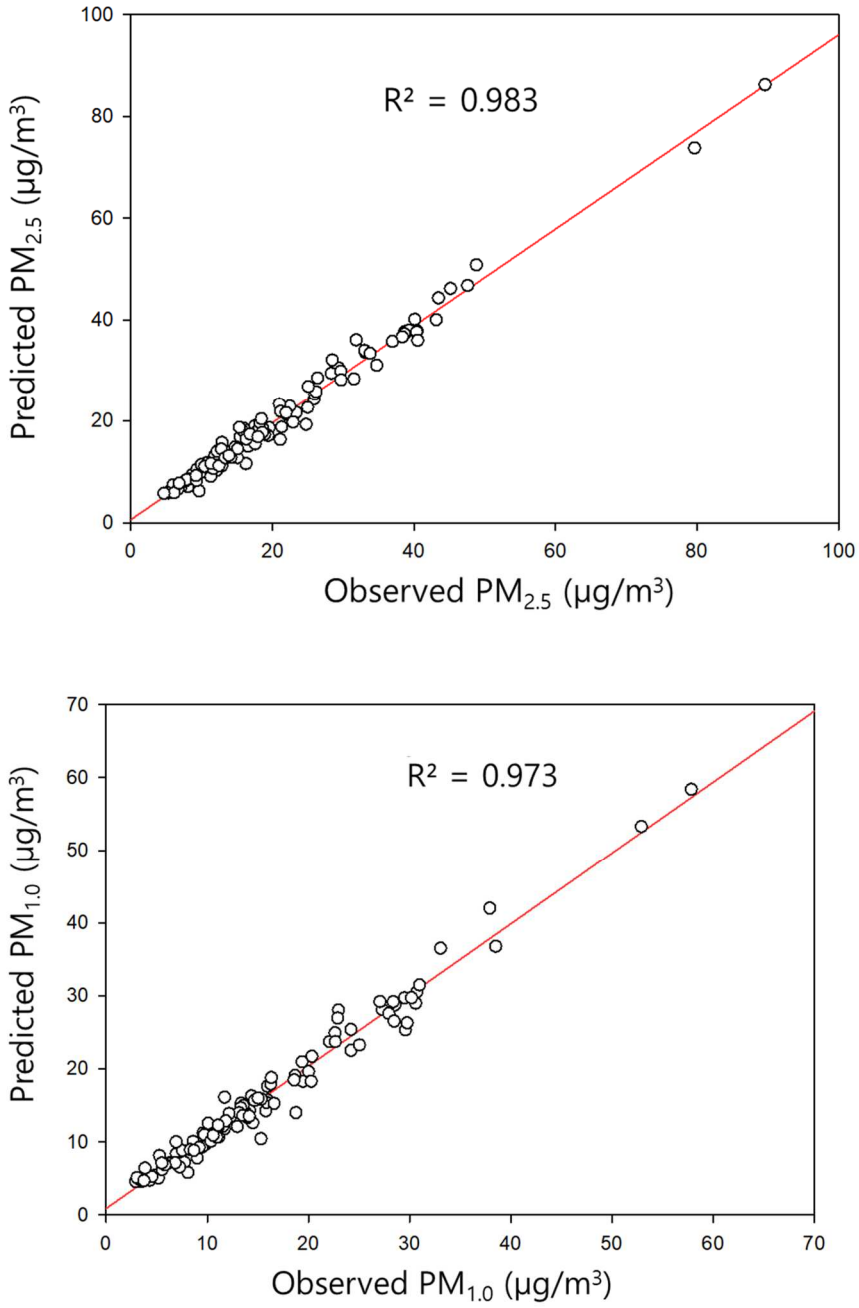

Figure S4 The plots that compare the mass concentration predicted by the PMF model with the observed mass concentration

국문초록

서울 $PM_{2.5}$와 $PM_{1.0}$의 오염원 추정과 산화 잠재력 평가

서울대학교 보건대학원
환경보건학과 환경보건학전공
김태연

$PM_{1.0}$은 인위적 과정에서 주로 배출되고 $PM_{2.5}$의 건강 영향에 대부분을 차지하기 때문에 $PM_{2.5}$뿐만 아니라 $PM_{1.0}$에 대한 연구의 필요성은 커지고 있다. 본 연구에서는 서울의 $PM_{2.5}$와 $PM_{1.0}$의 성분을 분석하고 dithiothreitol (DTT) 분석을 통해 산화 잠재력을 평가하였다. 또한, positive matrix factorization (PMF)을 통해 오염원을 추정하였고 conditional bivariate probability function (CBPF), cluster analysis, potential source contribution function (PSCF)를 통해 오염원들의 특징을 비교하였다. 서울에서 채취한 123개 시료의 평균 질량농도에서 $PM_{1.0}$ (15.1 μg/m^3)이 $PM_{2.5}$ (20.1 μg/m^3)의 약 75%를 차지하였다. 이는 이차 생성과 연소관련 오염원이 $PM_{2.5}$에 크게 기여하는 것을 나타낸다. Organic carbon (OC), SO_4^{2-}, NH_4^+는 $PM_{1.0}$에서 유의하게 큰 비율을 차지하고 있었고 지각 성분의 비율은 $PM_{2.5}$에서 유의하게 컸다. PMF 결과 10개의 오염원이 기여했으며, 각각의 오염원과 기여도(μg/m^3)는 다음과 같다($PM_{2.5}$, $PM_{1.0}$). 이차 질산염: 6.01 (29%), 5.23 (32%); 이차 황산염: 3.64 (17%), 3.48 (22%); 자동차: 2.71 (13%), 1.81 (11%);

생물성연소: 2.69 (13%), 2.03 (13%); 소각: 0.81 (3.8%), 0.69 (4.3%); 토양: 0.61 (2.9%), 0.30 (1.9%); 산업: 1.65 (7.8%), 0.40 (2.5%); 석탄연소: 1.77 (8.4%), 1.22 (7.6%); 기름연소: 0.40 (1.9%), 0.35 (2.2%); 노후 해염: 0.72 (3.4%), 0.64 (4.0%). 이차 생성 오염원(이차 질산염과 이차 황산염)은 $PM_{1.0}$에서 더 큰 기여도 비율을 차지했으며, 산업과 토양 오염원의 기여도 비율은 $PM_{2.5}$에서 더 높았다. 자동차 오염원에서는 도로 먼지로 인한 성분의 차이가 나타났다. CBPF는 서울 주변의 오염원 방향을 잘 나타내고 있었으며 많은 오염원들이 남쪽과 서쪽에 위치한 산업단지의 영향을 받는 것으로 나타났다. 클러스터 분석에서는 역궤적이 만주와 북한을 통해 유입될 때 생물성연소의 기여도가 높아졌고, 산둥성에서 유입되는 경우 이차 생성 오염원의 기여도가 증가했다. PSCF 결과에서도 주로 산둥성을 포함한 North China Plain이 이차 생성 오염원의 오염원 가능지역으로 나타났고 이 오염원들은 고농도 사례 시 기여도가 유의하게 증가하였다. 특히, North China Plain으로부터의 이차 황산염은 계절관리제기간 동안 고농도 사례 시 $PM_{1.0}$에 크게 기여했다. $PM_{2.5}$와 $PM_{1.0}$의 DTTv (nmol/min/m^3)는 각각 0.611, 0.588로 $PM_{2.5}$의 산화 잠재력의 대부분에 $PM_{1.0}$이 기여했다. Pearson 상관 분석에서 OC가 DTTv와 가장 높은 상관성을 보였다($PM_{2.5}$: r=0.873, $PM_{1.0}$: r=0.786). 다중 회귀분석에서 이차 질산염과 생물성연소는 $PM_{2.5}$와 $PM_{1.0}$에서 모두 DTTv를 설명하는 변수로 선택되었다. 이 결과에서 생물성연소는 산화 잠재력과 관련된 중요한 오염원이었고 이차 질산염은 이차 생성 과정의 영향을 나타냈다. 본 연구는 오염원과 산화 잠재력의 특성을 파악하기 위한 지속적인 $PM_{1.0}$ 연구의 필요성을 보여주었고, 서울에서 이차 생성과 생물성연소 오염원 관리의 필요성을 나타냈다.

주요 단어: $PM_{2.5}$, $PM_{1.0}$, PMF, PSCF, DTT 분석

학번: 2020-20432